ORNL/TM-2022/2590

Standardizing a Renewed Fission Product Yield Library and Related Covariances (Part II)

Marco T. Pigni

September 2022

OAK RIDGE National Laboratory

ORNL IS MANAGED BY UT-BATTELLE LLC FOR THE US DEPARTMENT OF ENERGY

ORNL/TM-2022/2590

Nuclear Energy and Fuel Cycle Division

Standardizing a Renewed Fission Product Yield Library and Related Covariances (Part II)

Marco T. Pigni

September 2022

Prepared by
OAK RIDGE NATIONAL LABORATORY
Oak Ridge, TN 37831
managed by
UT-Battelle LLC
for the
US DEPARTMENT OF ENERGY
under contract DE-AC05-00OR22725

CONTENTS

LIST OF FIGURES

ABBREVIATIONS

ENDF	Evaluated Nuclear Data File
FPY	fission product yield
ORNL	Oak Ridge National Laboratory

ACKNOWLEDGMENTS

This work was supported by the Nuclear Regulatory Commission (NRC)

ABSTRACT

A complete library of independent fission product yields including covariance information was generated by a sequential Bayesian methodology. The prior information consisted of independent fission product yields and branching ratios of the possible decay modes reported in the recently released ENDF/B-VIII.0 nuclear data library. The Bayesian procedure consisted of the adjustment of independent fission product yields to match the set of stable and long-lived cumulative yields reported in the ENDF/B-VIII.0 nuclear data library; in this work, these yields were considered as legacy values together with their uncertainties. According to the χ^2-metric, the results obtained by this methodology show a systematic improvement in terms of the agreement with legacy reported cumulative yields for the entire adjusted independent fission product yield library.

1. INTRODUCTION

Following the series of previous works [1][2][3][4] on fission product yield (FPY) evaluation data, this report describes the generation of a complete, independent FPY library including covariance information obtained by a sequential Bayesian update. The prior information used in the Bayesian procedure consisted of both independent FPYs and branching ratios of possible decay modes ($\beta^{\pm}$, β-n, isomeric transition, α-decay, ...) reported in the recently released ENDF/B-VIII.0 nuclear data library [5]. The Bayesian procedure comprised the adjustment of independent FPYs to match the set of stable and long-lived* cumulative yields reported in the ENDF/B-VIII.0 nuclear data library—which, in this work, were considered as "legacy" values together with their uncertainties. The Bayesian algorithm is an updated version of the methodology presented in Pigni, Francis, and Gauld [1]. Conversely, in this work, the adjustment of the independent FPY is performed only on stable and long-lived nuclei similarly to that documented in Kawano and Chadwick [6]. Although the uncertainties of cumulative FPYs along the decay chain are neglected in the updated adjustment procedure, the advantage is the reduction in the dimension related to the cumulative FPY matrix.

The scope of the work described in this report aligns with the work presented in Pigni et al. [1] and Francis et al. [2] and represents its completion, as independent FPY data including covariance information are generated over the entire set of nuclei and for all incident neutron energies available in the ENDF/B-VIII.0 nuclear data library. The goal is to generate independent FPY data to be used in depletion simulations to calculate fission product concentrations in agreement with the cumulative FPY reported in the ENDF/B-VIII.0 library. The possible disagreement with the legacy cumulative FPY is linked to the decay library and traces back to ENDF/B-VI release. In fact, the ENDF/B-VIII.0 FPY sub-library—with the exception of a new FPY evaluation for ^{239}Pu [6]—is based on the compilations developed by England and Rider, released in 1994 [7]. Namely, England and Rider produced a recommended set of independent and cumulative FPYs† based on a compiled list of open literature measurements and calculated charge distributions. This set was the basis for the FPY evaluations used in ENDF/B-VI library released in 1993 and was subsequently adopted by ENDF/B-VII.0, -VII.1, and -VIII.0 libraries released in 2006, 2011, and 2018, respectively. Since England and Rider's initial release of yield data, improved nuclear decay schemes have been adopted in decay sub-libraries following the ENDF/B-VI release. Therefore, the changes of the branching ratios for the possible decay modes in the decay library created inconsistencies between the legacy cumulative FPYs (ENDF/B-VIII.0) and current calculated data. Another important outcome implicitly generated by this approach is the generation of covariance data on the cumulative FPYs that are necessary for fission

*Nuclei with a half-life greater than 24 hours were selected.

†These evaluated data included uncertainties for both independent and cumulative yields but no covariance information.

product uncertainty quantification.

The following two sections provide a brief description of the methodology, focusing on the updated algorithm (Section 2.) and the results of the adjustment procedure for the entire set of nuclei (Section 3.). The summary and conclusions are presented in Section 5..

2. METHODOLOGY

The Bayesian algorithm used in the present work is an updated version of the algorithm presented in Pigni et al. [1] and developed by Kawano and Chadwick [6]. We refer to those references for a detailed description of the algorithm and, here, we briefly discuss the updates. First, one should highlight the dependence of the set of cumulative yields $\mathbf{C}$ to the decay library by the branching ratios b as well as the set of independent yields $\mathbf{I}$, starting from their relation,

$$C_i^{n+1} = I_i + \sum_j C_j^n \, b_{j\to i} \,, \tag{1}$$

where the index i refers to each independent and cumulative yields identified by the triplet (A, Z, M). Here, A and Z are the mass and charge number, respectively, whereas M represents the isomeric state ($M = 0$ for the ground state, $M = 1$ for the 1^{st} meta state). Together with the related fraction $b_{j\to i}$ of the precursor nucleus j to the daughter nucleus i, the index j specifies the decaying nucleus and corresponding decay mode (β^-, β-n, isomeric transition, ...) for the formation of the nucleus labeled i. For a stable or very-long nucleus, the related cumulative yield C can be found by iterating Eq. (1) until convergence[‡] is found for C_i^n starting from $C_i^0 = I_i$ with no need of solving time-dependent coupled equations [6]. The Bayesian update procedure was restricted to fit legacy cumulative yields related to stable or long-lived nuclei. In this regard, in addition to the Bayesian equations—for instance Eqs. (6–8) in Ref. [1])—used to impose the physical constraints to the independent FPYs, the adjusted values of independent yields $\mathbf{I}'$ and related covariance matrix $\mathbf{P}'$ were computed by the following set of equations:

$$\begin{aligned} \mathbf{P}' &= \mathbf{P} - \mathbf{P}\mathbf{S}^{\mathrm{t}}(\mathbf{S}\mathbf{P}\mathbf{S}^{\mathrm{t}} + \mathbf{Z})^{-1}\mathbf{S}\mathbf{P} \,, \\ \mathbf{I}' &= \mathbf{I} + \mathbf{P}'\mathbf{S}^{\mathrm{t}}\mathbf{Z}^{-1}(\boldsymbol{\zeta} - \mathbf{C}(\mathbf{I})) \,, \end{aligned} \tag{2}$$

where $\mathbf{P}$ is the covariance matrix (diagonal in this specific case) of $\mathbf{I}$ generated from ENDF/B-VIII.0 uncertainties. The evaluated cumulative yields $\boldsymbol{\zeta}$ and related (diagonal) covariance matrix $\mathbf{Z}$ in the ENDF/B-VIII.0 library are restricted to stable and long-lived cumulative yields. Therefore, the dimension $(n \times m)$ of the sensitivity matrix $\mathbf{S}$ is determined by the dimension of the vector $\mathbf{I}$ (i.e., m) and the dimension of the vector $\boldsymbol{\zeta}$ or matrix $\mathbf{Z}$ (i.e., n).

3. RESULTS

In Figs. 1–50, the ratios of adjusted cumulative yields (in blue) to ENDF/B-VIII.0 legacy values (in purple) are plotted for all available nuclei at each incident neutron energy. A systematic improvement in the agreement with the legacy cumulative yields is shown together with a reduction of the related uncertainties of the cumulative yields obtained from the independent FPY covariance matrix. The reduction in the uncertainties can be understood by the negative correlations of the independent FPY covariance matrix generated in the

[‡]Convergence within 10^{-5} precision is usually reached by 10 iterations.

Bayesian procedure. These plots refer to stable or long-lived cumulative yields with a magnitude $< 10^{-3}$ and, because the cumulative yields are plotted as a function of their mass A in the case of metastable nuclei, the plots show two data points for the same mass. The case for the highest discrepancy is reported for ^{239}Pu at 14 MeV incident neutron energy in Fig. 25. The vector of adjusted independent FPY ($\mathbf{I}'$ in Eq. (2)) was constrained to sum to 2 (two fragments per fission) within 10^{-5} precision. However, a large tolerance for the other two physical constraints such as the total charge and prompt neutron emission was given so as to be comparable to the ENDF/B-VIII.0 FPY compilations.

4. REPOSITORY

The `FISSPRO` code written to generate these results was stored on a GitHub repository found at the following link `https://code-int.ornl.gov/xtp/fisspro`. This repository contains the source files, including the installation cmake file, the scripts to generate the entire FPY library, as well as the LaTeX files and figures for this report. The repository consists of five directories, the contents of which are described below.

- **`inputs`** contains 51 input files whose name clearly identifies the nucleus, isotope, and energy (e.g., `input.u235thermal`). These files list independent and cumulative FPYs with related uncertainties plus a file (`origen.revxx.decay.data`) containing the decay information. All the information is taken from the ENDF/B-VIII.0 nuclear data library.

- **`report`** contains the LaTeX files to generate this report, including a sub-directory `figs` for the figures.

- **`runs`** contains the results of the calculations generated by running the bash script `runall.sh` linked from the **`../scripts`** directory. The bash script assumes to find the executable `fisspro` in the **`../build`** directory and the decay file `origen.revxx.decay.data` in the **`../inputs`** directory. After running the calculations with the command `./runall.sh`, the results consist of 51 directories with names easily link-able to the input files (e.g., `u235thermal`). There is also a bash script `plot_stable.sh` used to generate plots of the ratios which requires the gnuplot file `plot_stable.gp`. Both files are also linked from the **`../scripts`** directory.

- **`scripts`** contains the `bash` scripts to be used in the **`../runs`** directory.

- **`src`** contains the source files written in Fortran90

The repository also includes a `CMakeLists.txt` file used for the usual `cmake` configuration. This consists of creating a build directory with the command `mkdir build`, followed by the shell commands `cd build` and `cmake ../`. The configuration will configure the Makefile with the following compiler options `-Wall -O0 -g -bounds-check -fbacktrace -finit-real=zero -fno-range-check -ffpe-trap=invalid,zero,overflow -fno-align-commons -lblas -llapack`.

5. SUMMARY AND CONCLUSIONS

The entire ENDF/B-VIII.0 independent FPY library was adjusted to consistently match the legacy FPY cumulative yields. In doing so, the decay information reported in the ENDF/B-VIII.0 library was used. In addition to the adjusted FPY, covariance information (uncertainty and related correlations) was generated. The results of this work can be used for both uncertainty quantification in depletion calculations and adjustment analyses [4] as implemented in the SCALE code. According to the χ^2-metric, the results obtained by this work show a systematic improvement in the agreement with legacy reported cumulative yields for the entire adjusted independent fission product yield library. These results were stored in a GitHub repository including source and input files.

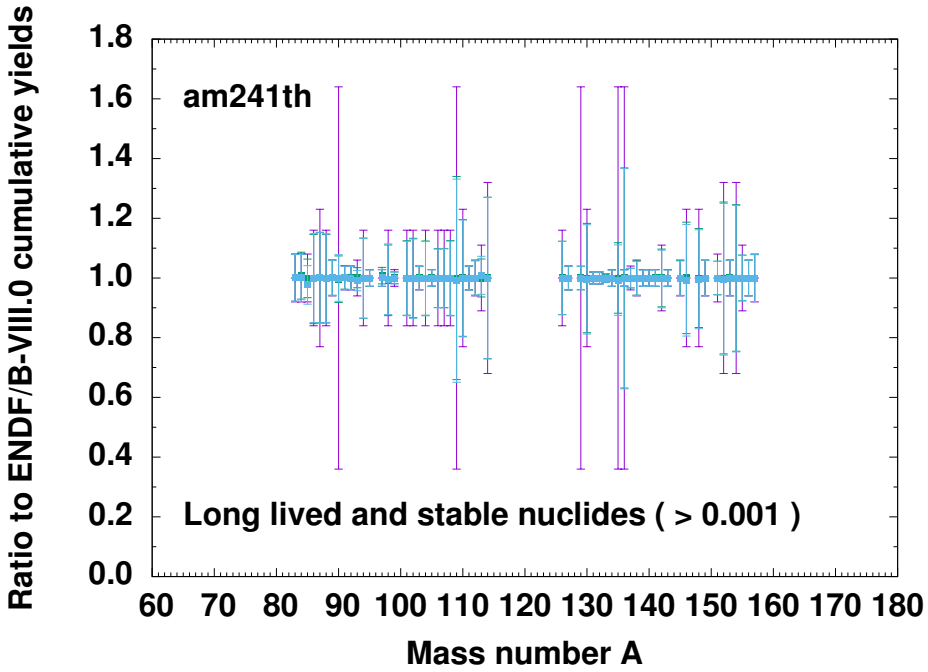

Figure 1. Ratios of stable and long-lived cumulative yields of magnitude $>10^{-3}$ fitted to ENDF/B-VIII.0 library for ^{241}Am at thermal neutron energy.

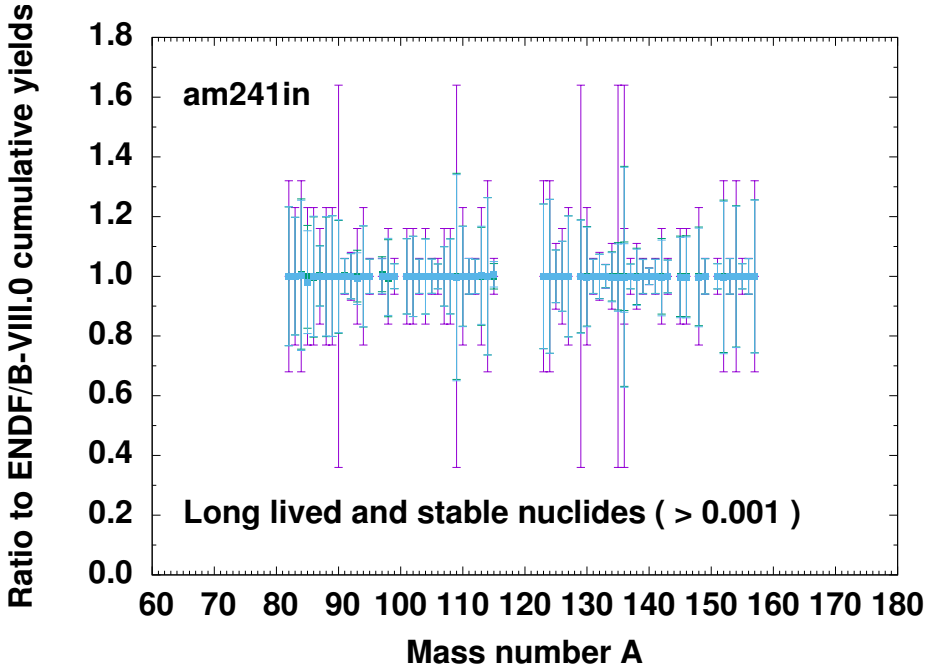

Figure 2. Ratios stable and long-lived cumulative yields of magnitude $>10^{-3}$ fitted to ENDF/B-VIII.0 library for ^{241}Am at 500 keV neutron energy.

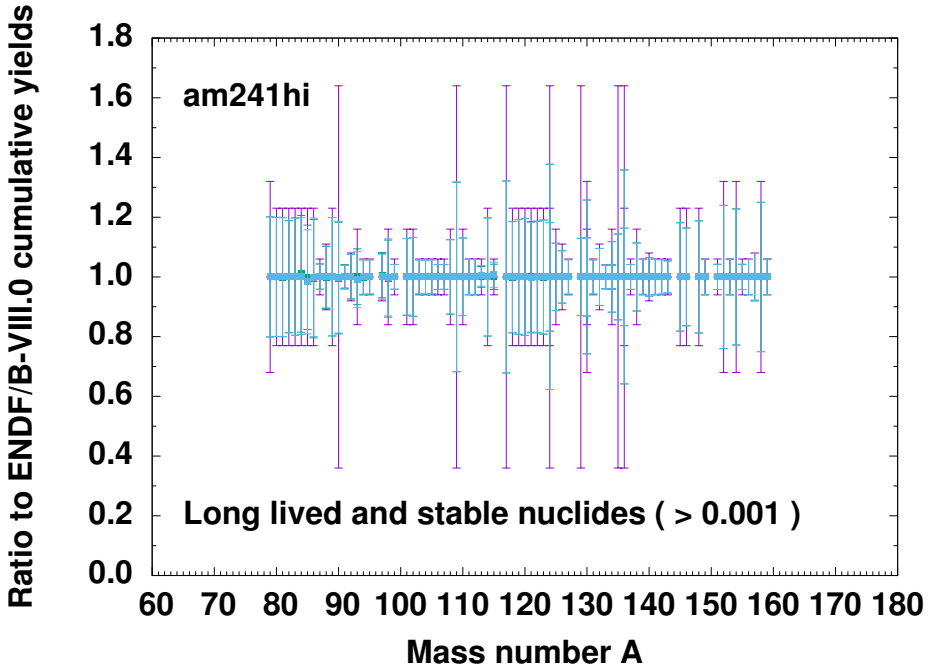

Figure 3. Ratios of stable and long-lived cumulative yields of magnitude $>10^{-3}$ fitted to ENDF/B-VIII.0 library for ^{241}Am at 14 MeV neutron energy.

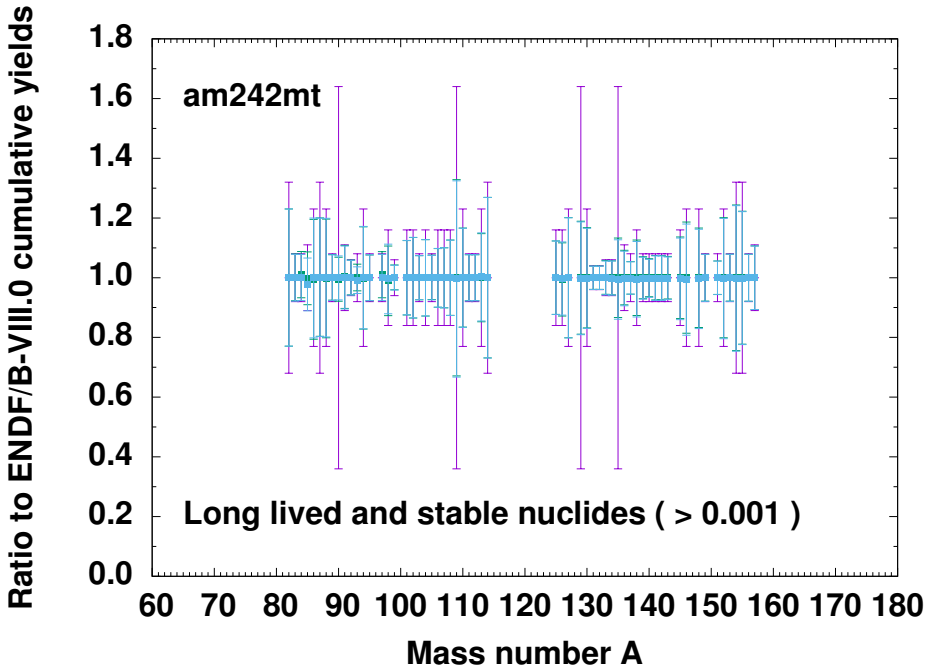

Figure 4. Ratios of stable and long-lived cumulative yields of magnitude $>10^{-3}$ fitted to ENDF/B-VIII.0 library for ^{242m}Am at thermal neutron energy.

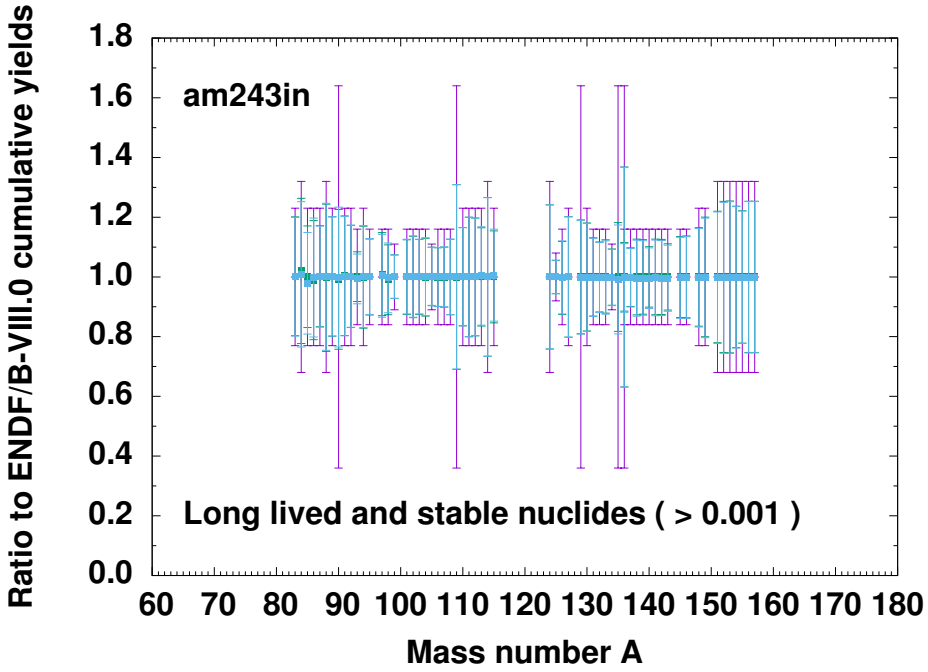

Figure 5. Ratios of stable and long-lived cumulative yields of magnitude $>10^{-3}$ fitted to ENDF/B-VIII.0 library for ^{243}Am at 500 keV neutron energy.

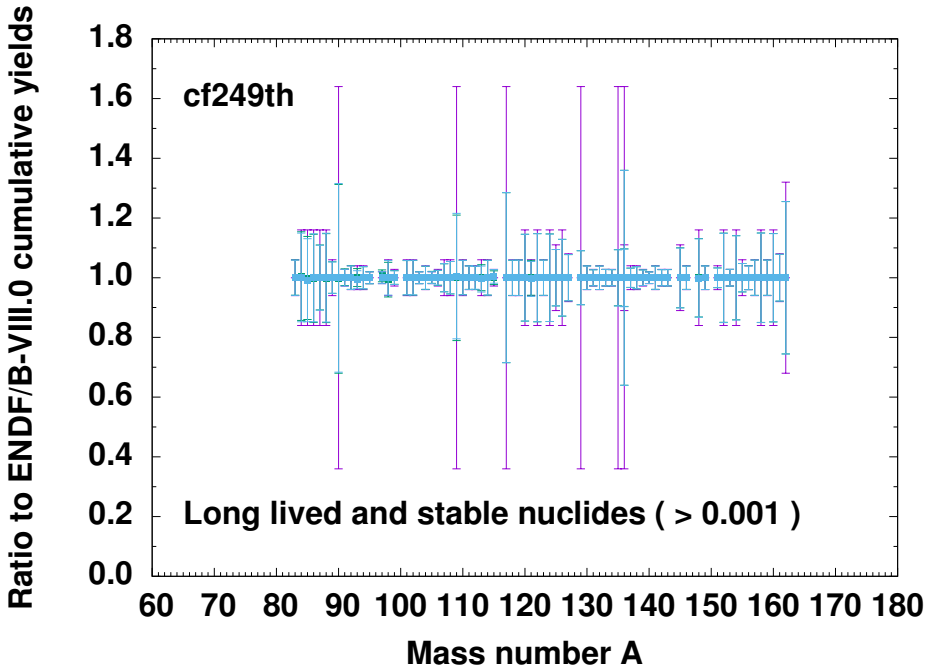

Figure 6. Ratios of stable and long-lived cumulative yields of magnitude $>10^{-3}$ fitted to ENDF/B-VIII.0 library for ^{249}Cf at thermal neutron energy.

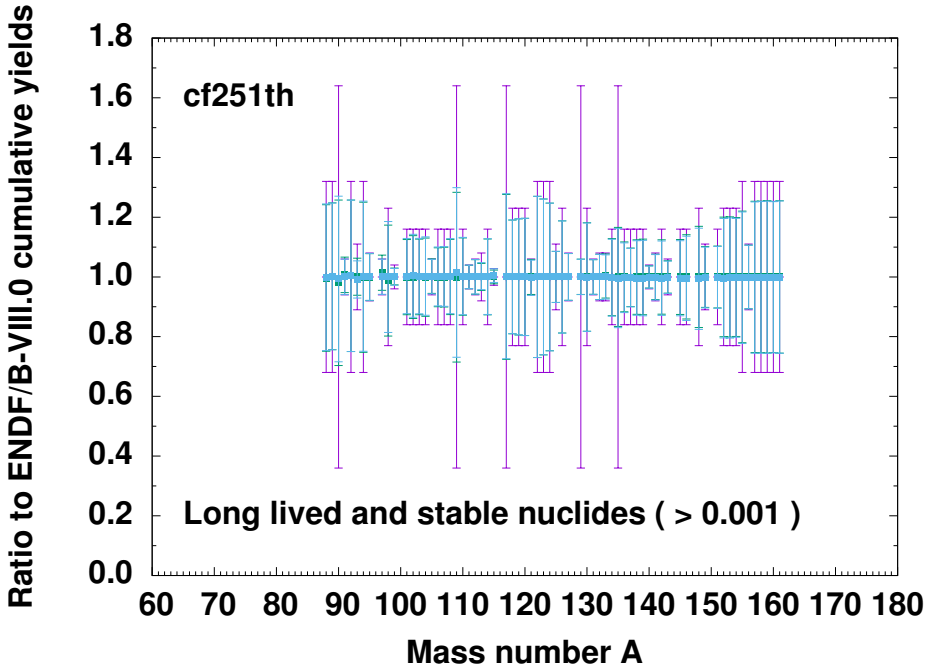

Figure 7. Ratios of stable and long-lived cumulative yields of magnitude $>10^{-3}$ fitted to ENDF/B-VIII.0 library for ^{251}Cf at thermal neutron energy.

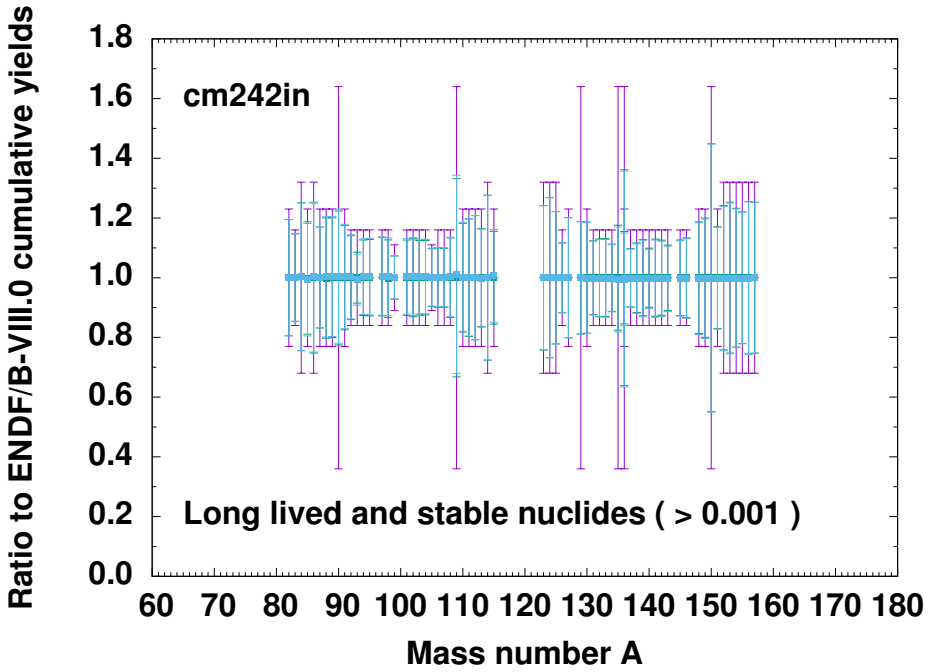

Figure 8. Ratios of stable and long-lived cumulative yields of magnitude $>10^{-3}$ fitted to ENDF/B-VIII.0 library for ^{242}Cm at 500 keV neutron energy.

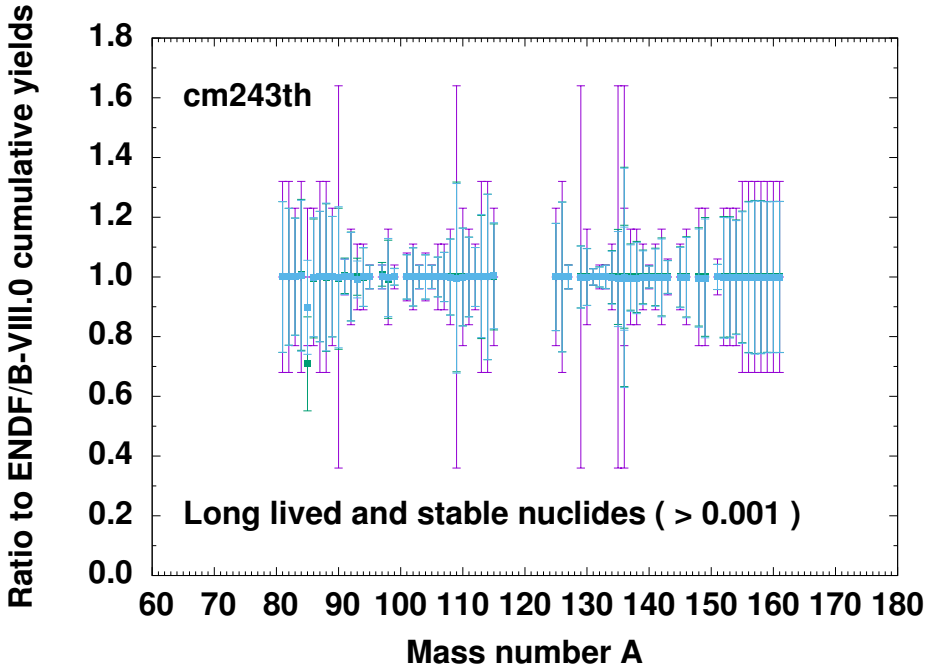

Figure 9. Ratios of stable and long-lived cumulative yields of magnitude $>10^{-3}$ fitted to ENDF/B-VIII.0 library for ^{243}Cm at thermal neutron energy.

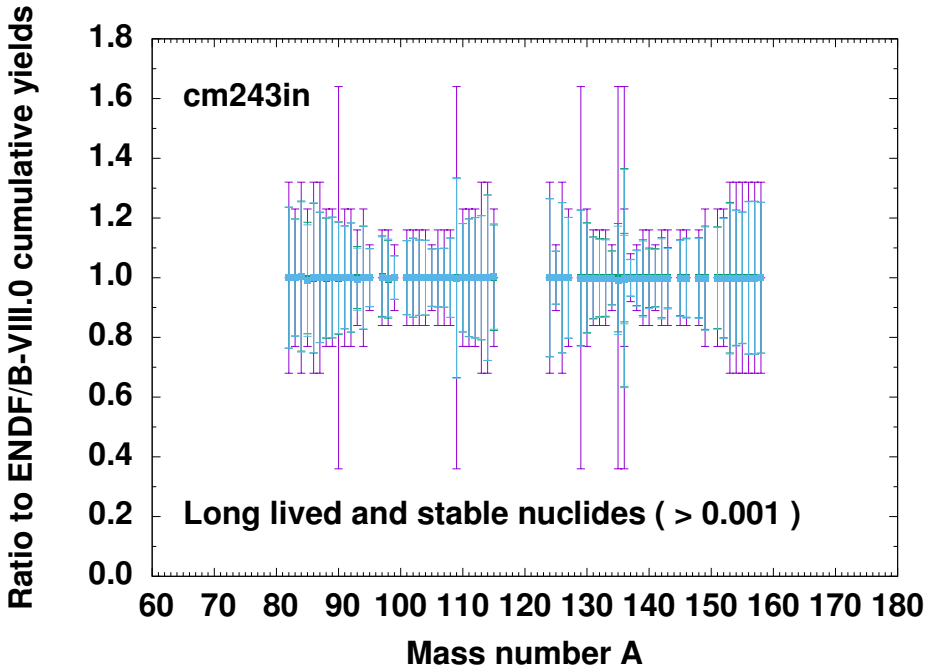

Figure 10. Ratios of stable and long-lived cumulative yields of magnitude $>10^{-3}$ fitted to ENDF/B-VIII.0 library for ^{243}Cm at 500 keV neutron energy.

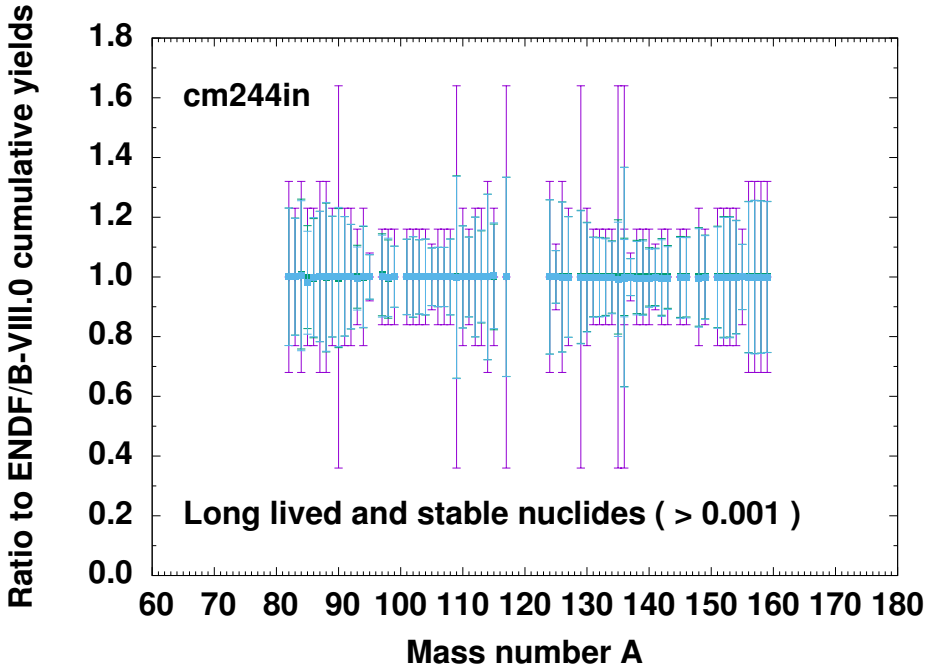

Figure 11. Ratios of stable and long-lived cumulative yields of magnitude $>10^{-3}$ fitted to ENDF/B-VIII.0 library for ^{244}Cm at 500 keV neutron energy.

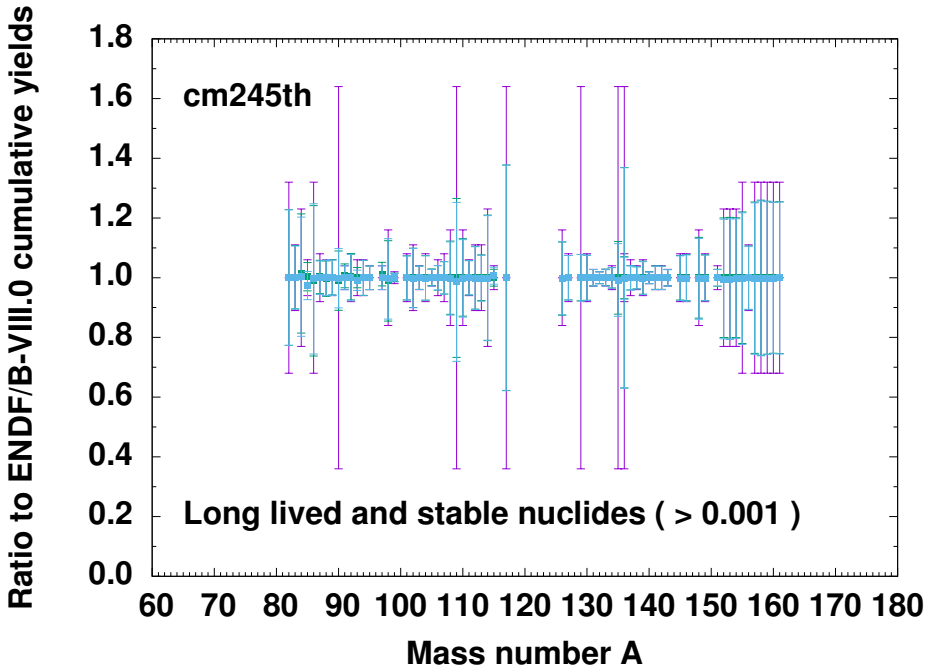

Figure 12. Ratios of stable and long-lived cumulative yields of magnitude $>10^{-3}$ fitted to ENDF/B-VIII.0 library for ^{245}Cm at thermal neutron energy.

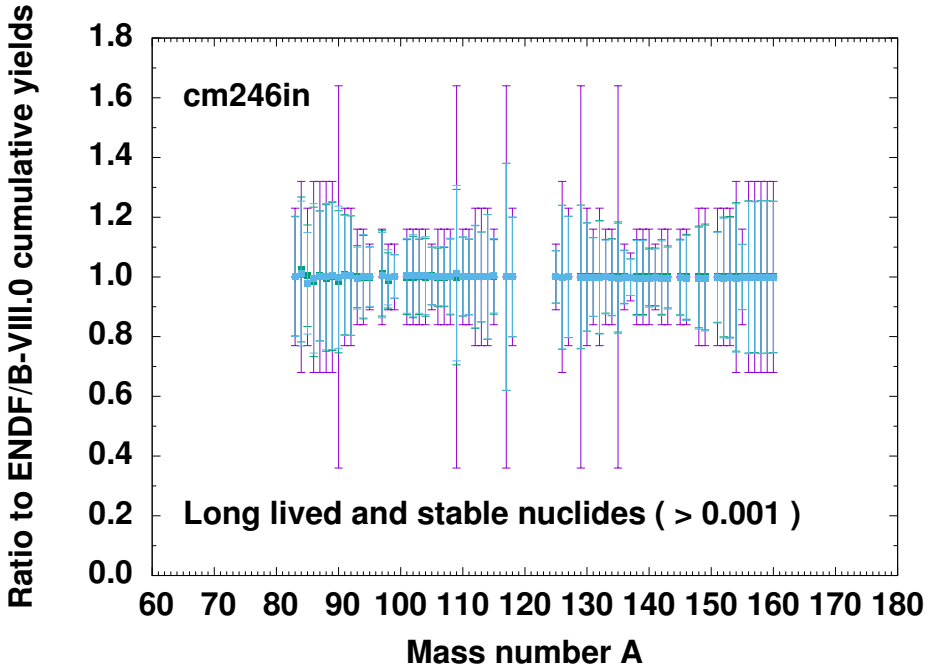

Figure 13. Ratios of stable and long-lived cumulative yields of magnitude $>10^{-3}$ fitted to ENDF/B-VIII.0 library for ^{246}Cm at 500 keV neutron energy.

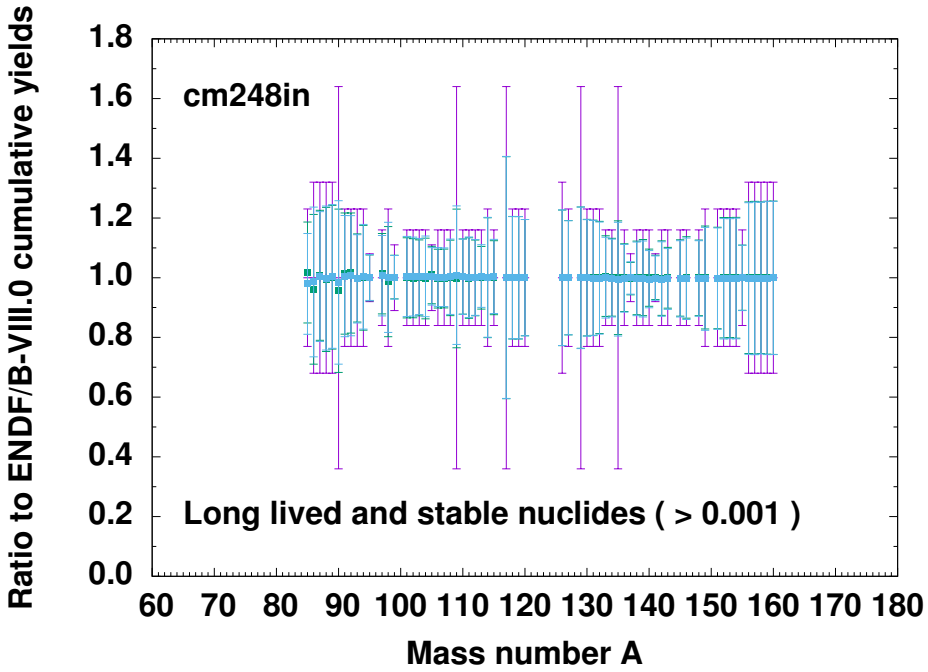

Figure 14. Ratios of stable and long-lived cumulative yields of magnitude $>10^{-3}$ fitted to ENDF/B-VIII.0 library for ^{248}Cm at thermal neutron energy.

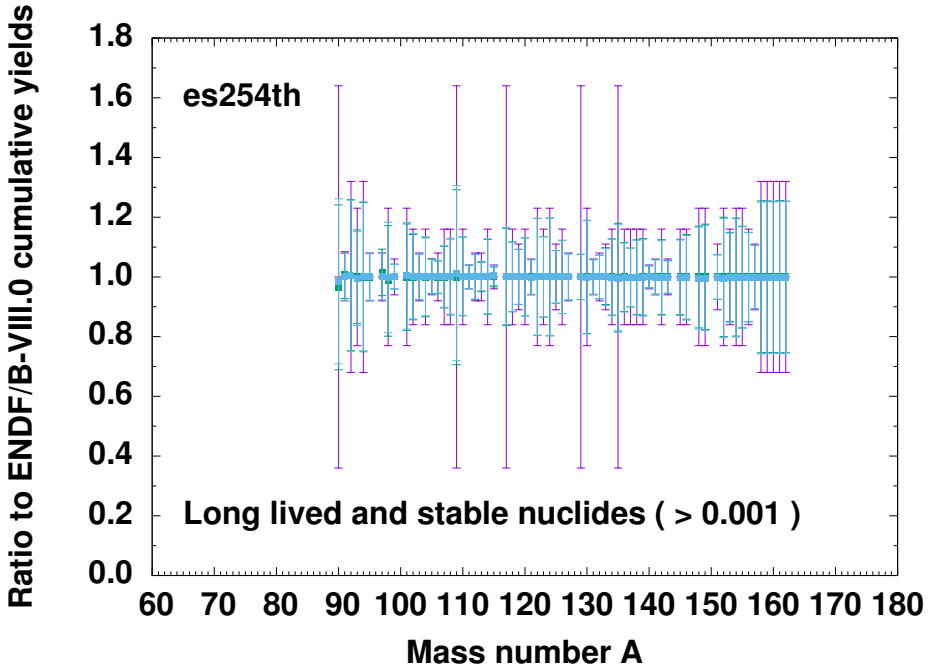

Figure 15. Ratios of stable and long-lived cumulative yields of magnitude $>10^{-3}$ fitted to ENDF/B-VIII.0 library for ^{254}Es at thermal neutron energy.

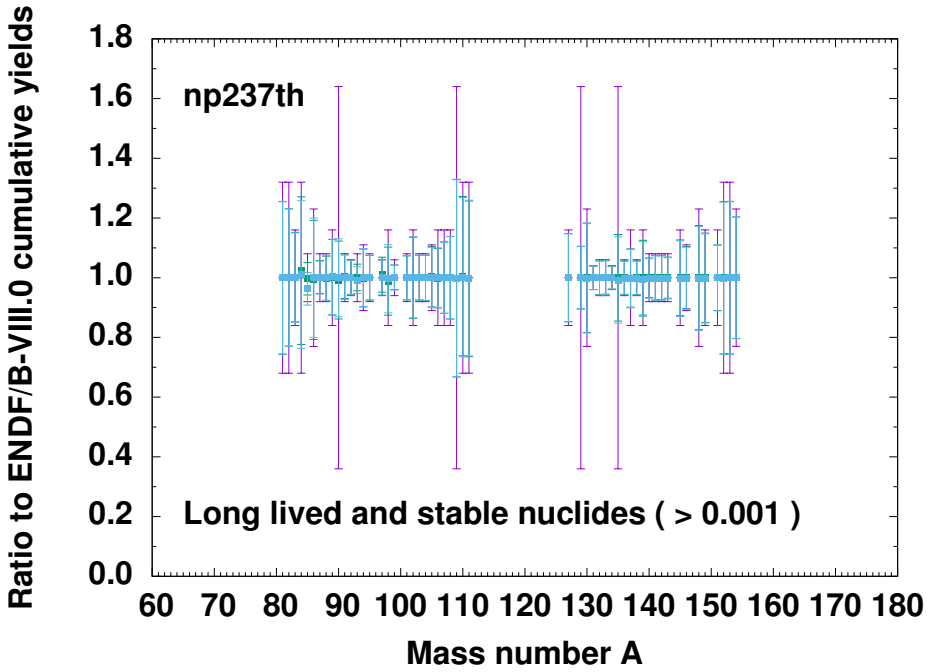

Figure 16. Ratios of stable and long-lived cumulative yields of magnitude $>10^{-3}$ fitted to ENDF/B-VIII.0 library for ^{237}Np at thermal neutron energy.

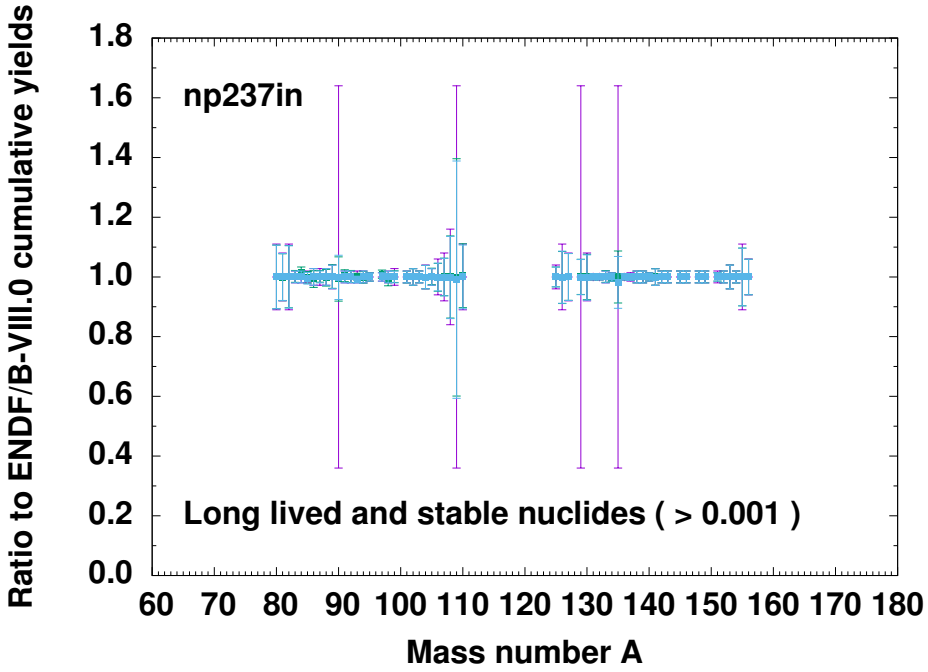

Figure 17. Ratios of stable and long-lived cumulative yields of magnitude $>10^{-3}$ fitted to ENDF/B-VIII.0 library for ^{237}Np at 500 keV neutron energy.

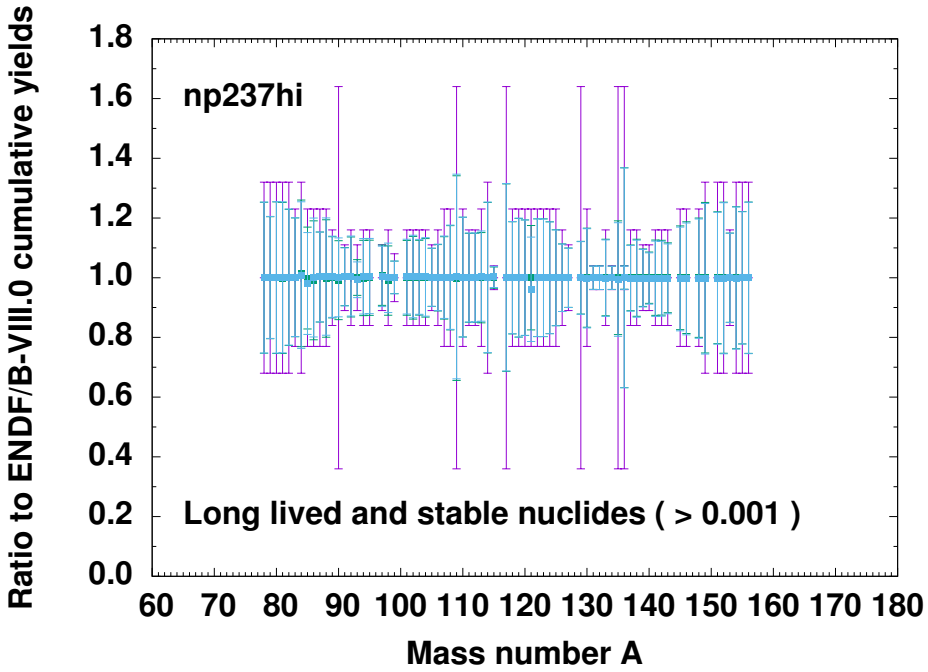

Figure 18. Ratios of stable and long-lived cumulative yields of magnitude $>10^{-3}$ fitted to ENDF/B-VIII.0 library for ^{237}Np at 14 MeV neutron energy.

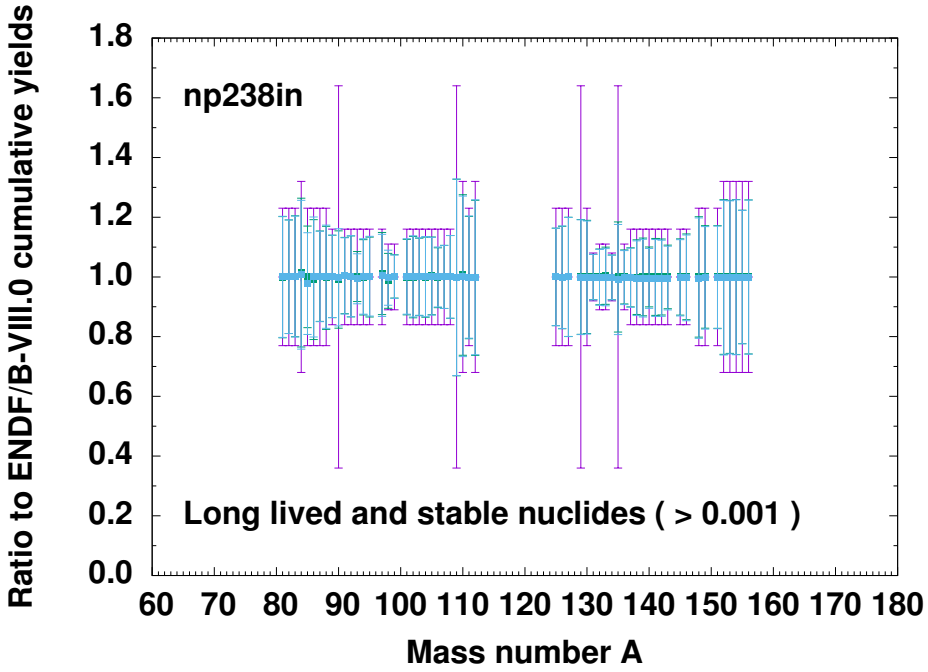

Figure 19. Ratios of stable and long-lived cumulative yields of magnitude $>10^{-3}$ fitted to ENDF/B-VIII.0 library for ^{238}Np at 500 keV neutron energy.

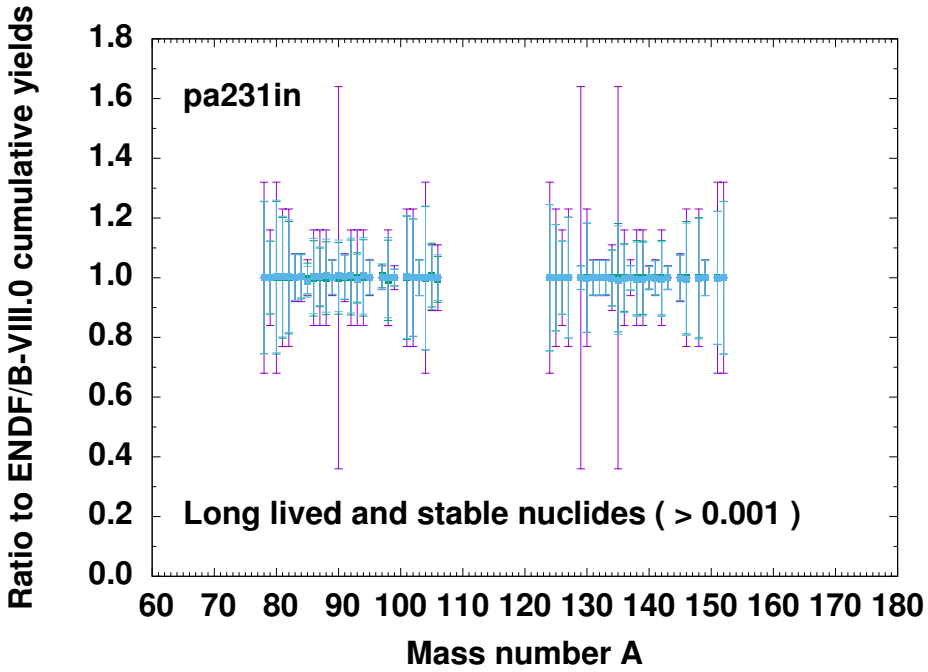

Figure 20. Ratios of stable and long-lived cumulative yields of magnitude $>10^{-3}$ fitted to ENDF/B-VIII.0 library for ^{241}Am at 500 keV neutron energy.

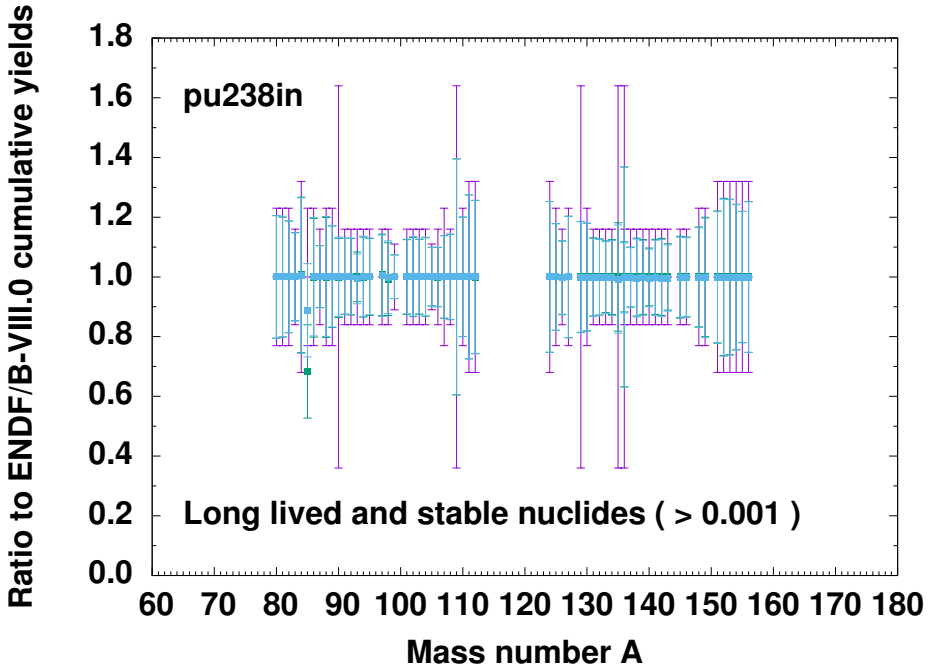

Figure 21. Ratios of stable and long-lived cumulative yields of magnitude $>10^{-3}$ fitted to ENDF/B-VIII.0 library for ^{238}Pu at 500 keV neutron energy.

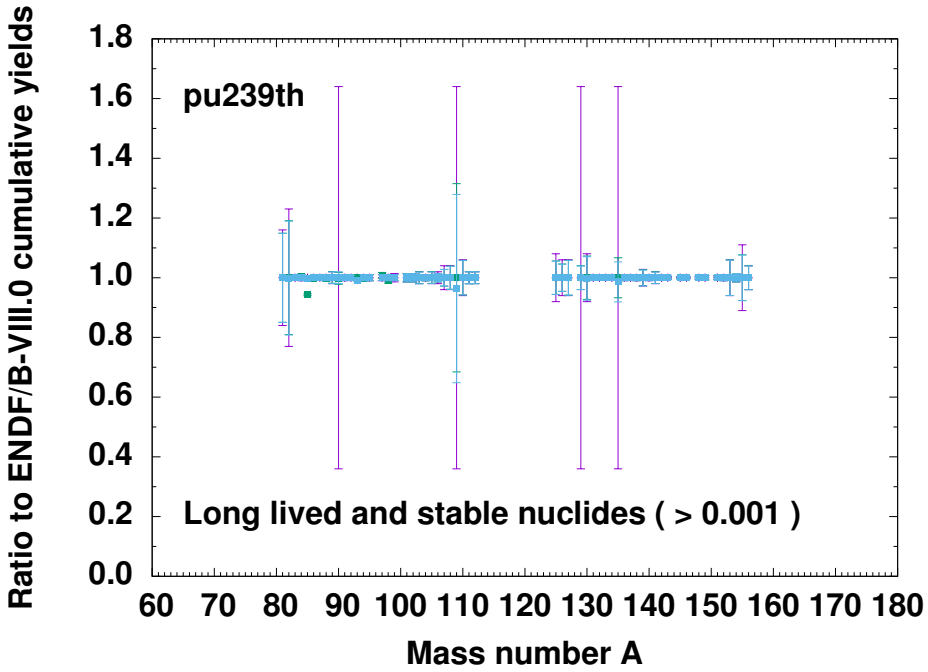

Figure 22. Ratios of stable and long-lived cumulative yields of magnitude $>10^{-3}$ fitted to ENDF/B-VIII.0 library for ^{239}Pu at thermal neutron energy.

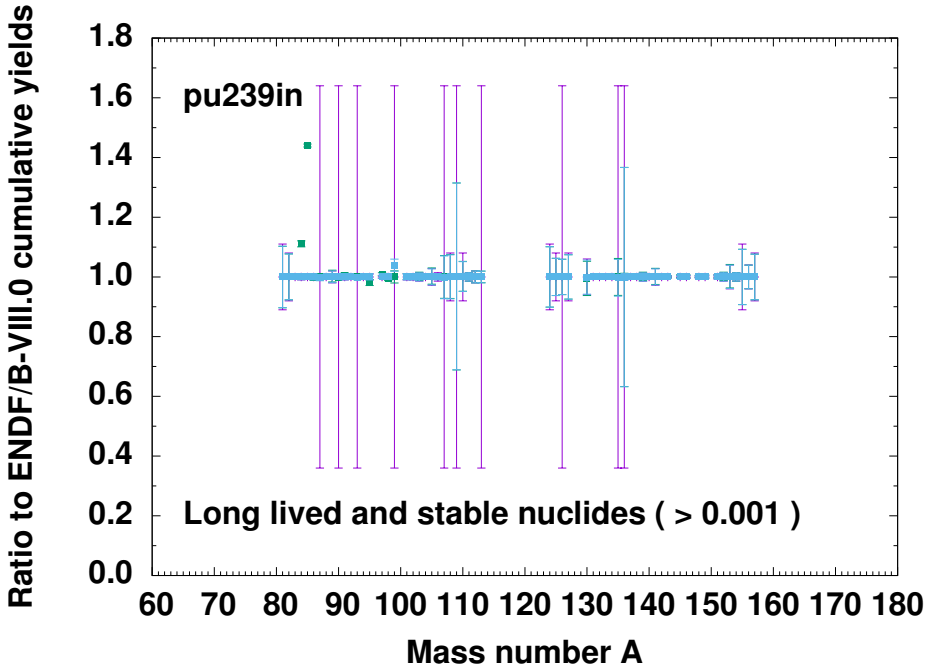

Figure 23. Ratios of stable and long-lived cumulative yields of magnitude $>10^{-3}$ fitted to ENDF/B-VIII.0 library for ^{239}Pu at 500 keV neutron energy.

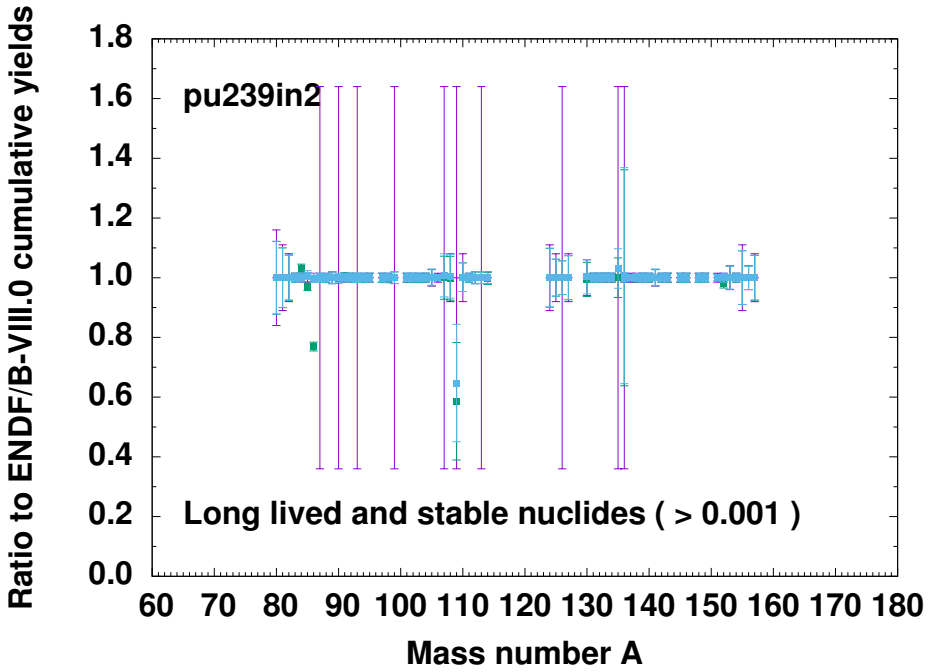

Figure 24. Ratios of stable and long-lived cumulative yields of magnitude $>10^{-3}$ fitted to ENDF/B-VIII.0 library for ^{239}Pu at 2 MeV neutron energy.

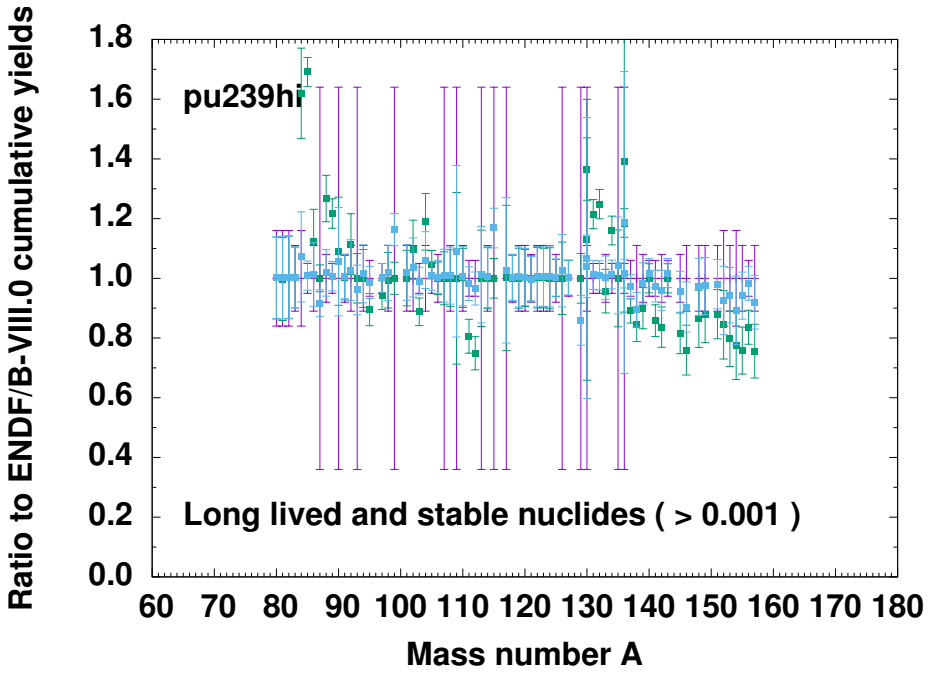

Figure 25. Ratios of stable and long-lived cumulative yields of magnitude $>10^{-3}$ fitted to ENDF/B-VIII.0 library for ^{239}Pu at 14 MeV neutron energy.

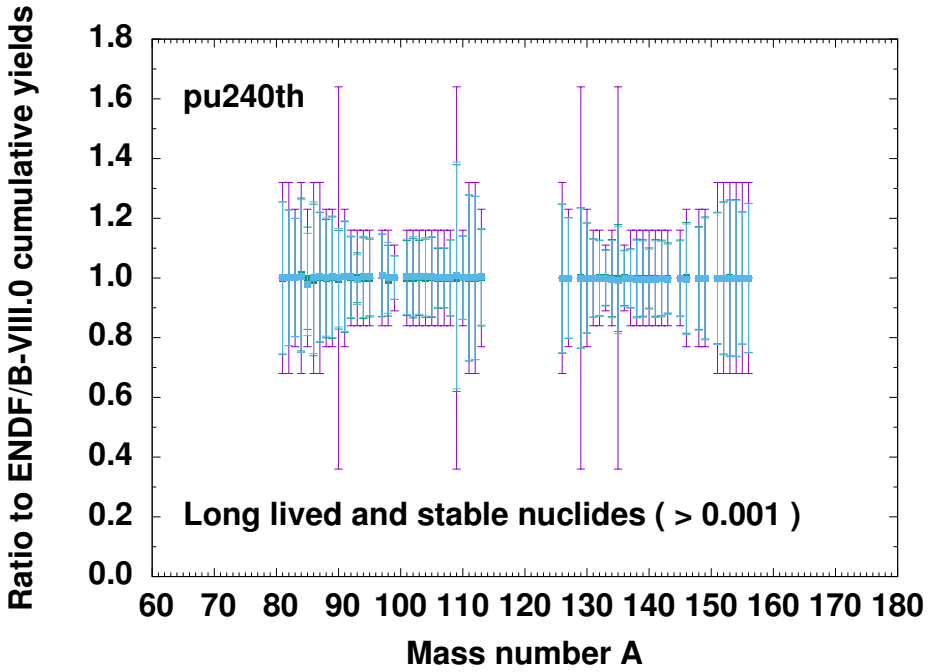

Figure 26. Ratios of stable and long-lived cumulative yields of magnitude $>10^{-3}$ fitted to ENDF/B-VIII.0 library for ^{240}Pu at thermal neutron energy.

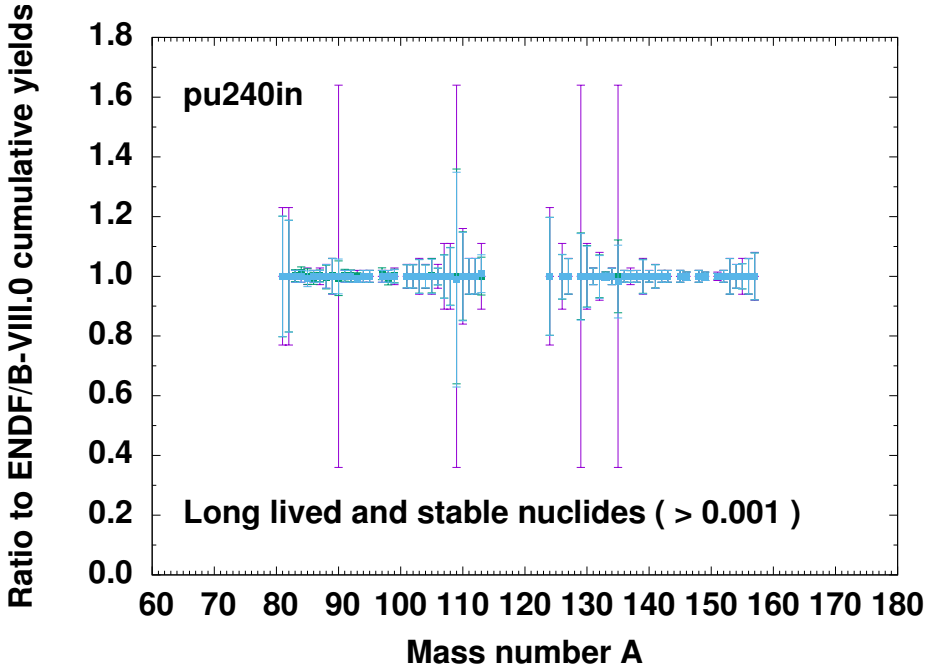

Figure 27. Ratios of stable and long-lived cumulative yields of magnitude $>10^{-3}$ fitted to ENDF/B-VIII.0 library for ^{240}Pu at 500 keV neutron energy.

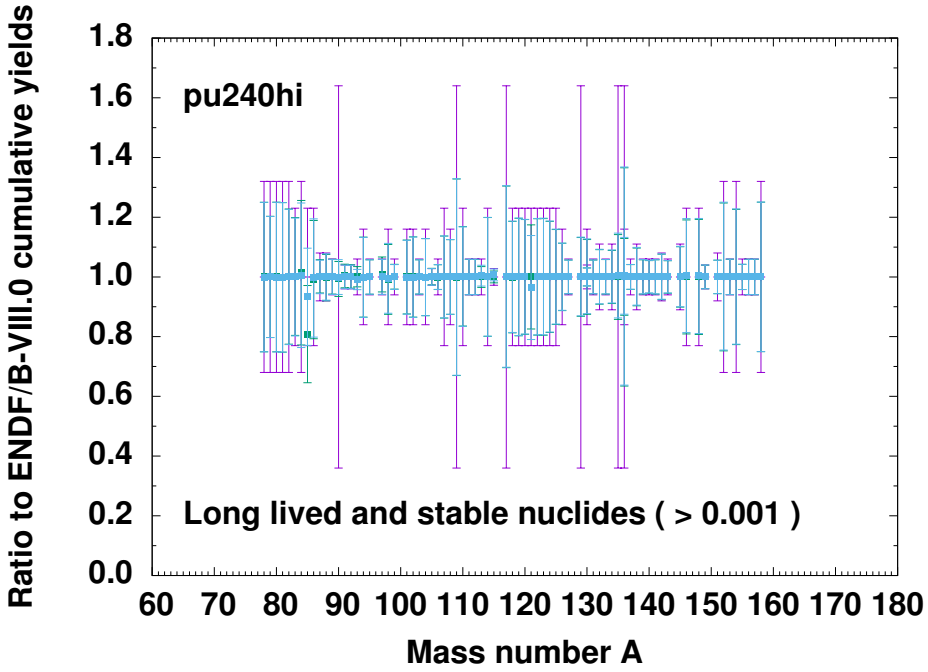

Figure 28. Ratios of stable and long-lived cumulative yields of magnitude $>10^{-3}$ fitted to ENDF/B-VIII.0 library for ^{240}Pu at 14 MeV neutron energy.

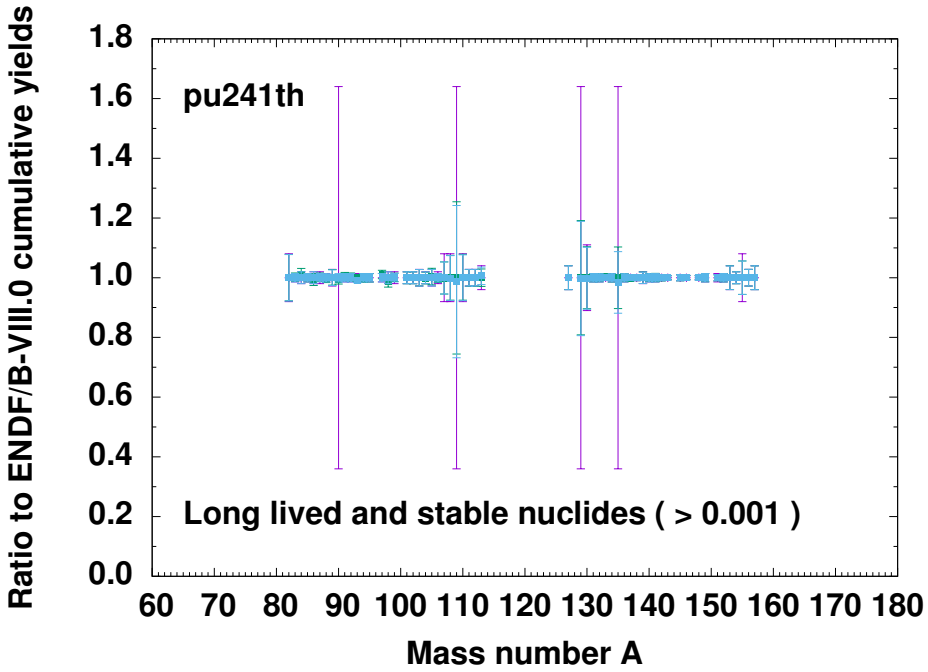

Figure 29. Ratios of stable and long-lived cumulative yields of magnitude $>10^{-3}$ fitted to ENDF/B-VIII.0 library for ^{241}Pu at thermal neutron energy.

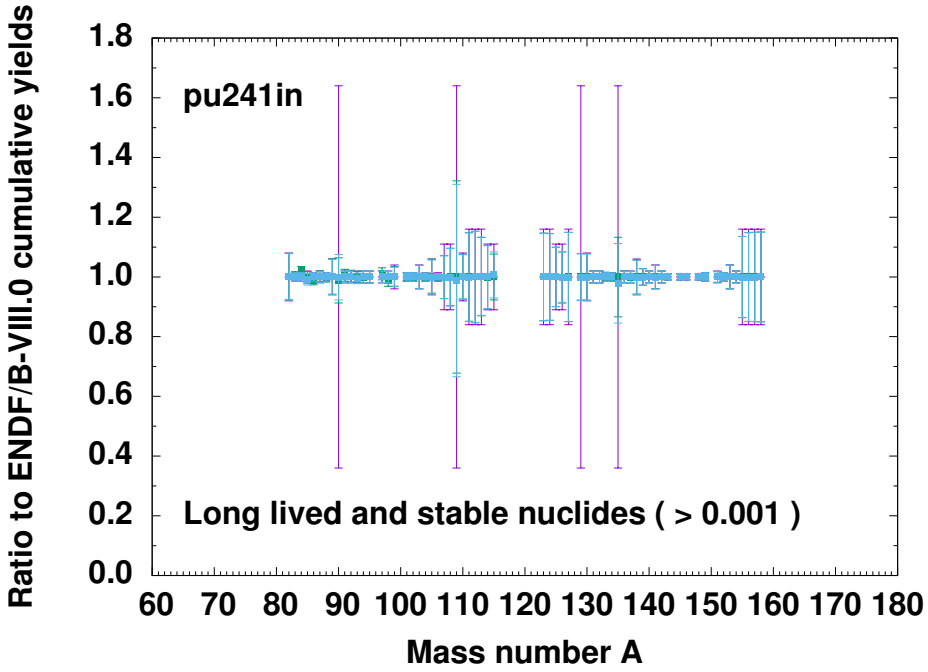

Figure 30. Ratios of stable and long-lived cumulative yields of magnitude $>10^{-3}$ fitted to ENDF/B-VIII.0 library for ^{241}Pu at 500 keV neutron energy.

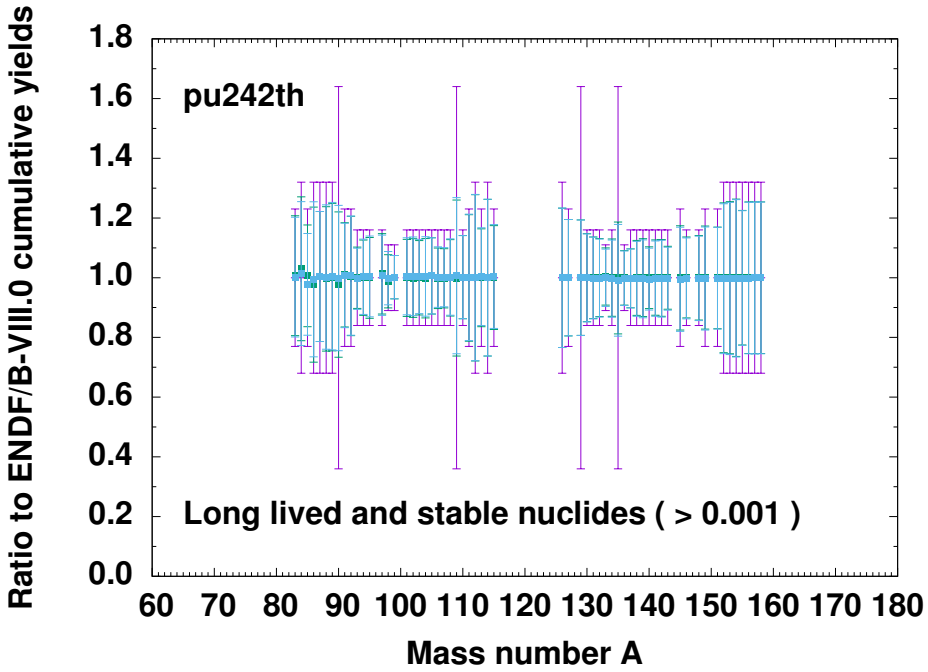

Figure 31. Ratios of stable and long-lived cumulative yields of magnitude $>10^{-3}$ fitted to ENDF/B-VIII.0 library for ^{242}Pu at thermal neutron energy.

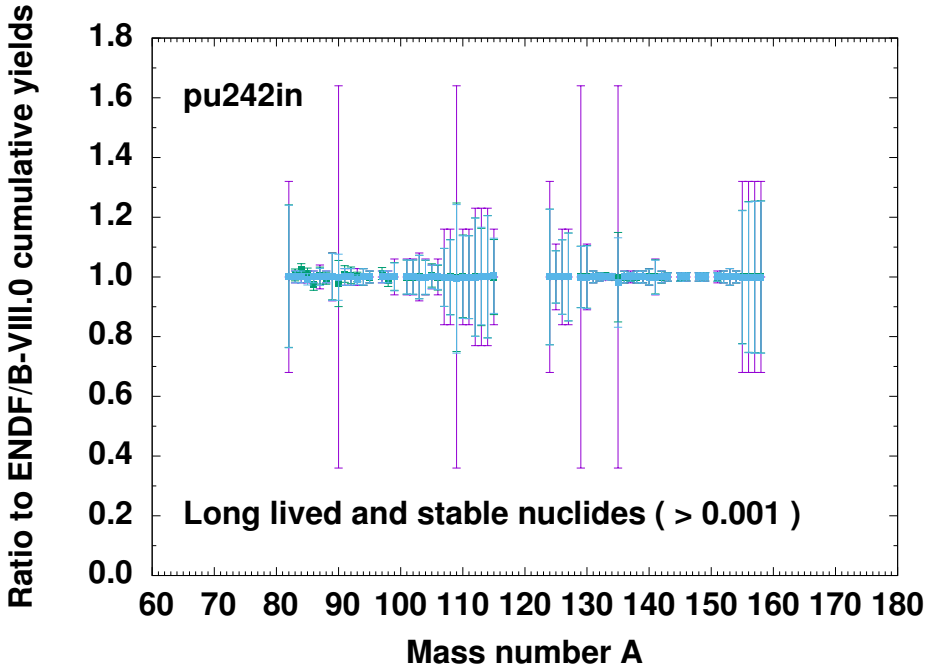

Figure 32. Ratios of stable and long-lived cumulative yields of magnitude $>10^{-3}$ fitted to ENDF/B-VIII.0 library for ^{242}Pu at 500 keV neutron energy.

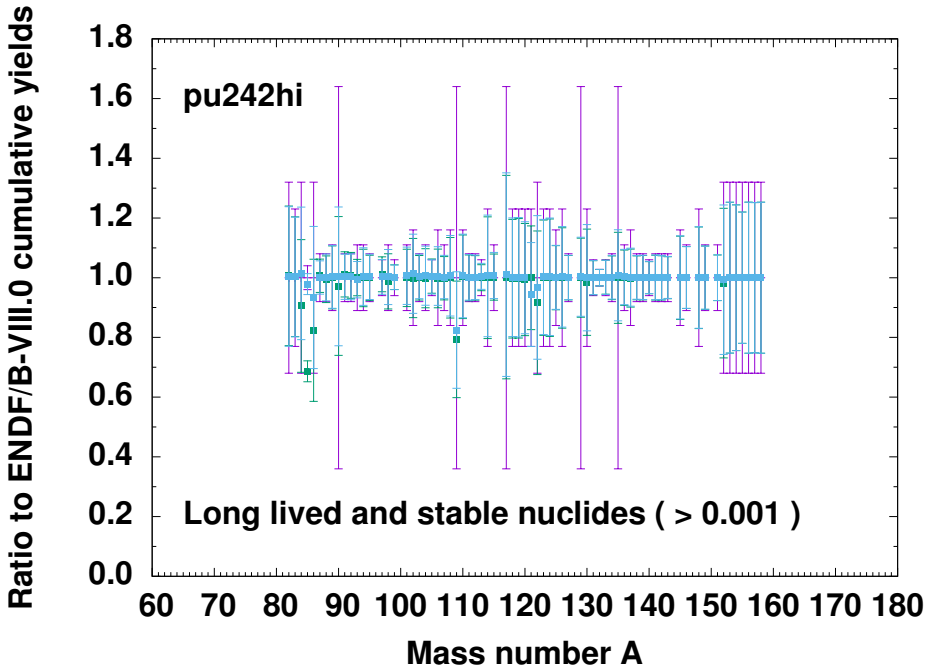

Figure 33. Ratios of stable and long-lived cumulative yields of magnitude $>10^{-3}$ fitted to ENDF/B-VIII.0 library for ^{242}Pu at 14 MeV neutron energy.

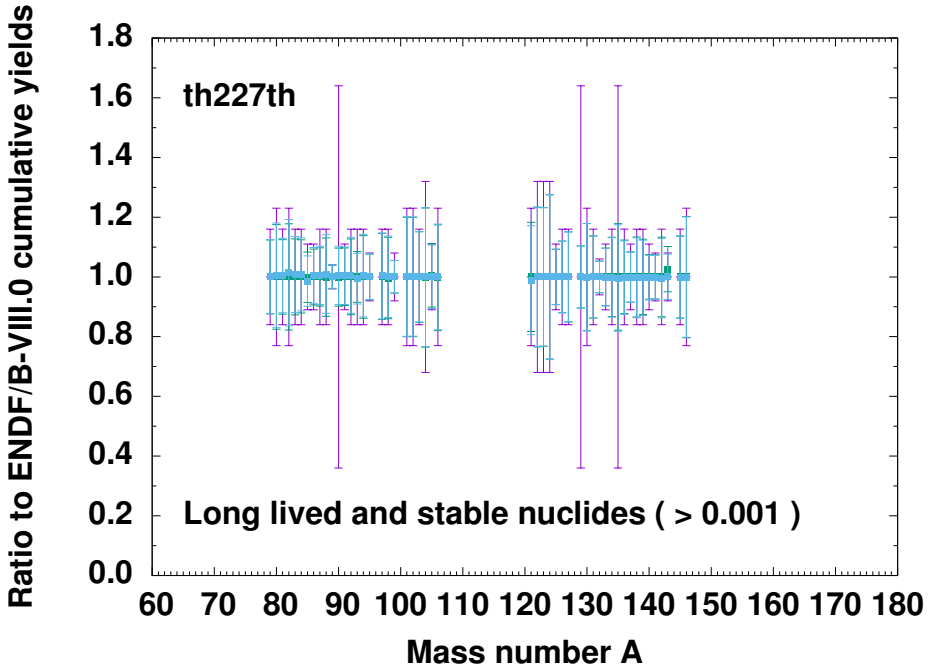

Figure 34. Ratios of stable and long-lived cumulative yields of magnitude $>10^{-3}$ fitted to ENDF/B-VIII.0 library for ^{227}Th at thermal neutron energy.

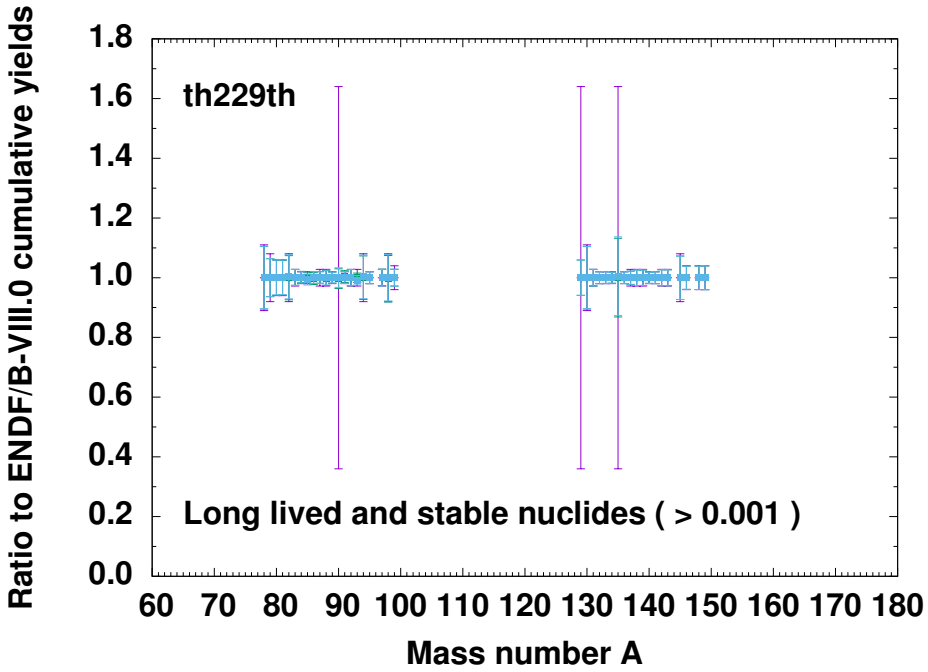

Figure 35. Ratios of stable and long-lived cumulative yields of magnitude $>10^{-3}$ fitted to ENDF/B-VIII.0 library for ^{229}Th at thermal neutron energy.

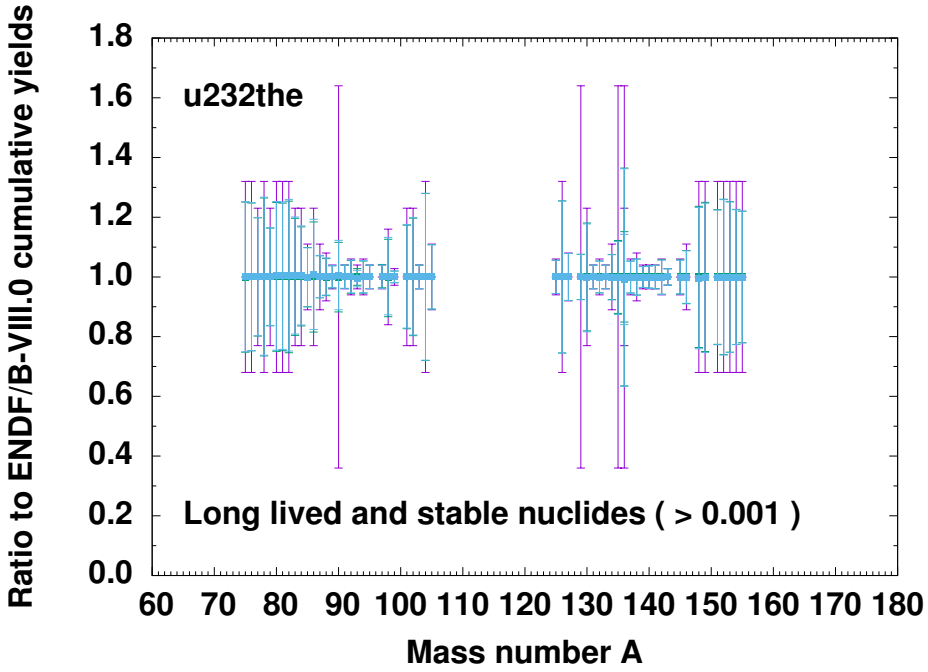

Figure 36. Ratios of stable and long-lived cumulative yields of magnitude $>10^{-3}$ fitted to ENDF/B-VIII.0 library for ^{232}Th at thermal neutron energy.

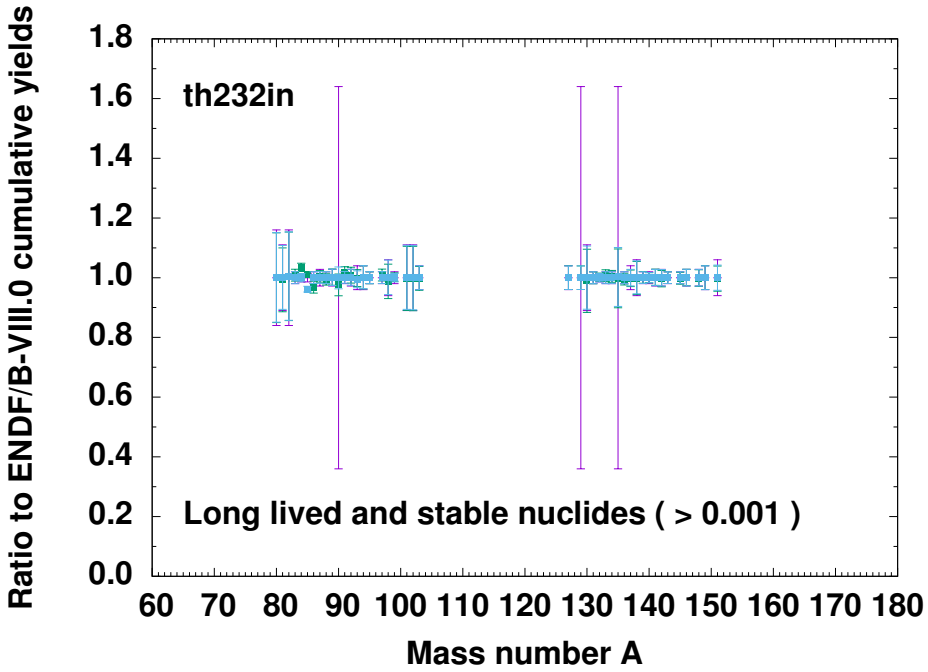

Figure 37. Ratios of stable and long-lived cumulative yields of magnitude $>10^{-3}$ fitted to ENDF/B-VIII.0 library for ^{232}Th at 500 keV neutron energy.

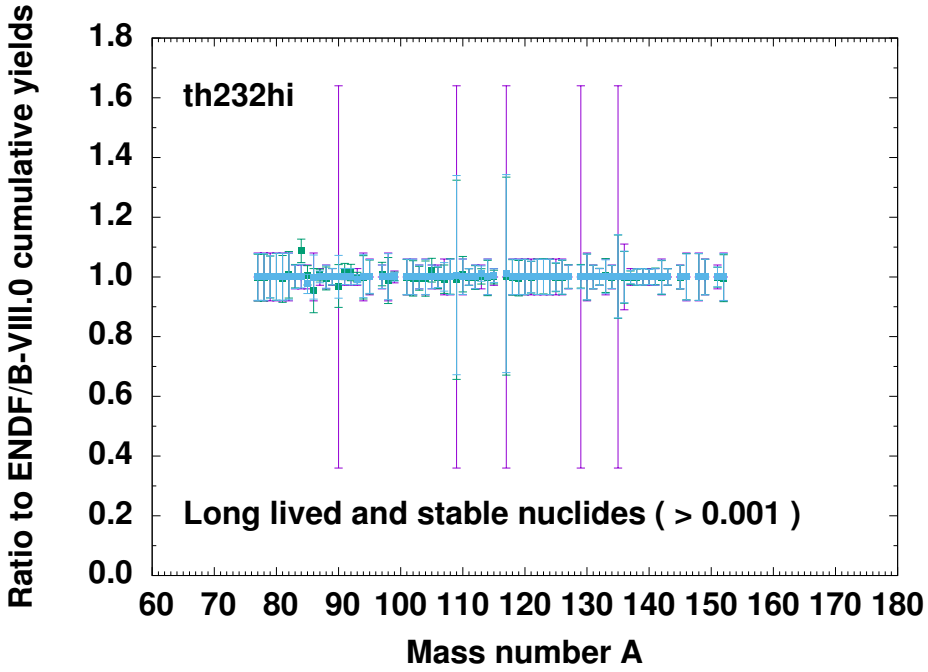

Figure 38. Ratios of stable and long-lived cumulative yields of magnitude $>10^{-3}$ fitted to ENDF/B-VIII.0 library for ^{232}Th at 14 MeV neutron energy.

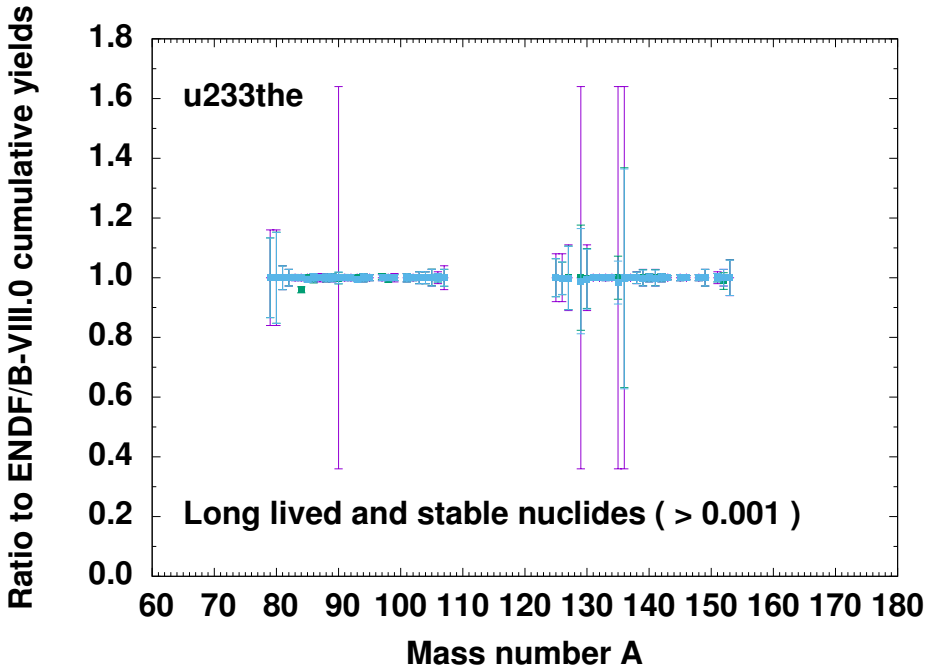

Figure 39. Ratios of stable and long-lived cumulative yields of magnitude $>10^{-3}$ fitted to ENDF/B-VIII.0 library for ^{233}U at thermal neutron energy.

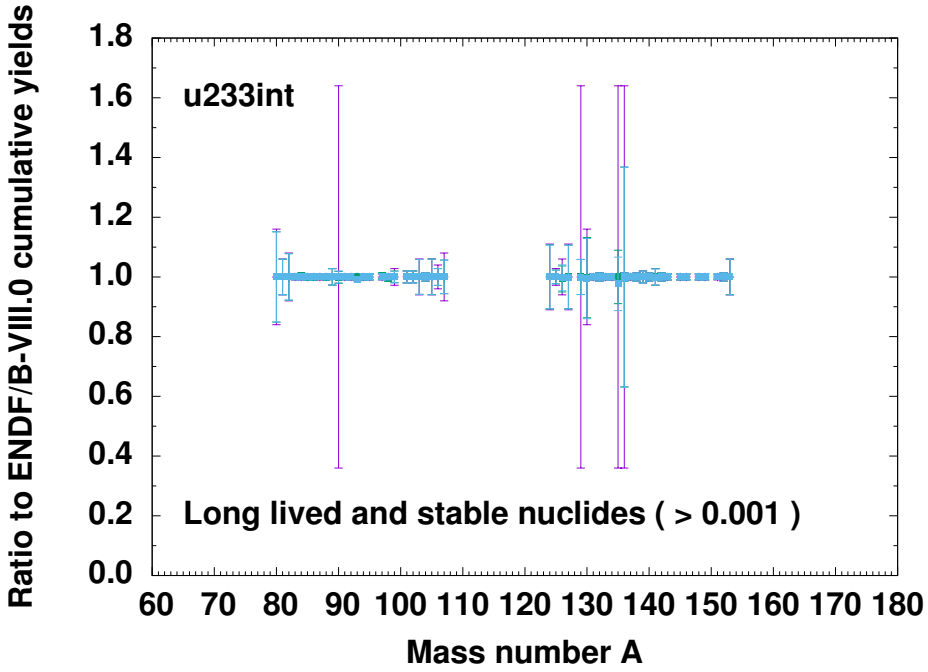

Figure 40. Ratios of stable and long-lived cumulative yields of magnitude $>10^{-3}$ fitted to ENDF/B-VIII.0 library for ^{233}U at 500 keV neutron energy.

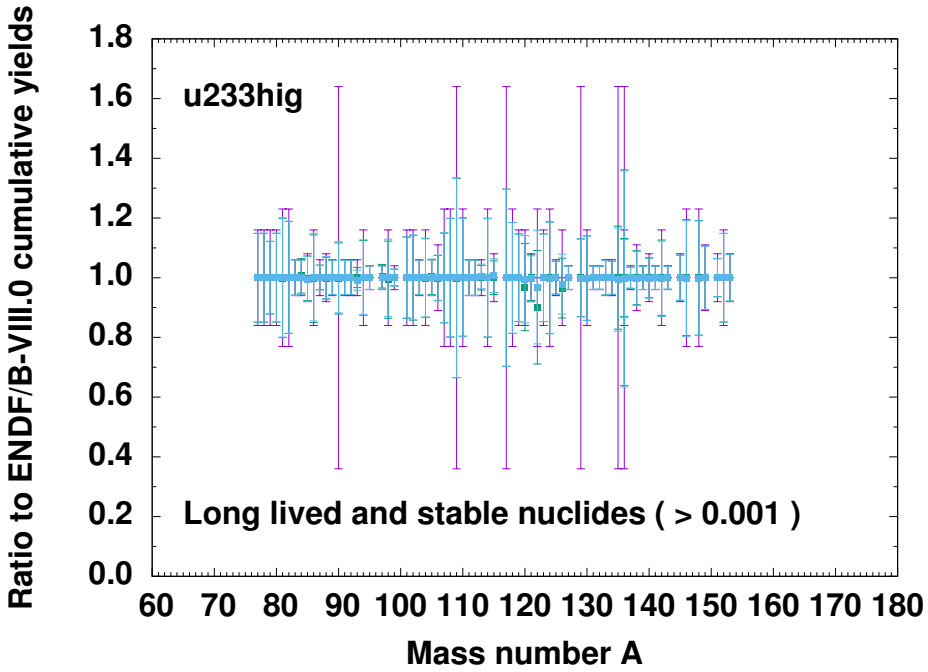

Figure 41. Ratios of stable and long-lived cumulative yields of magnitude $>10^{-3}$ fitted to ENDF/B-VIII.0 library for ^{233}U at 14 MeV neutron energy.

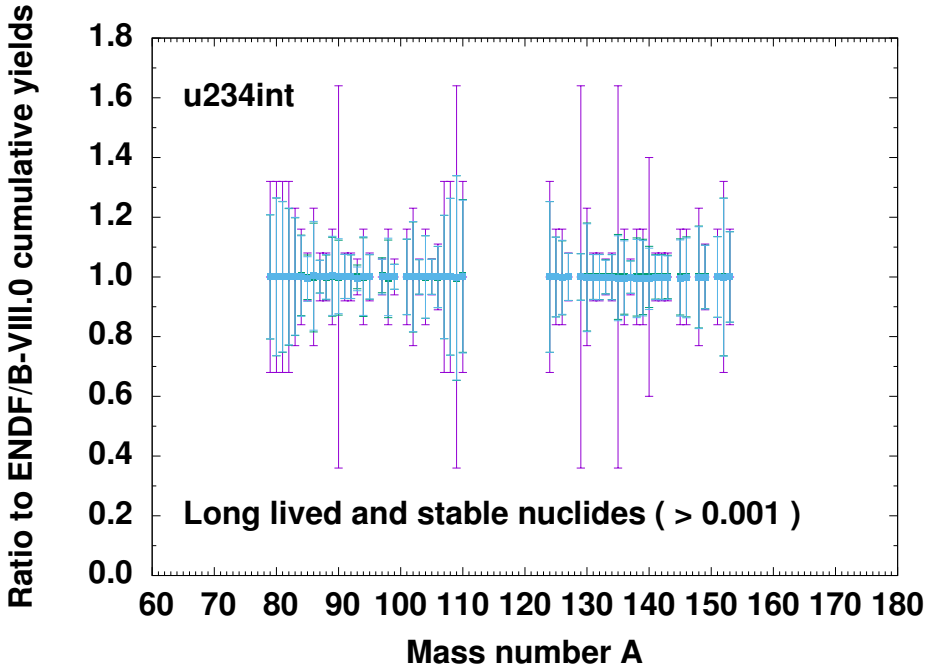

Figure 42. Ratios of adjusted stable and long-lived cumulative yields of magnitude >10^{-3} fitted to ENDF/B-VIII.0 library for ^{234}U at 500 keV neutron energy.

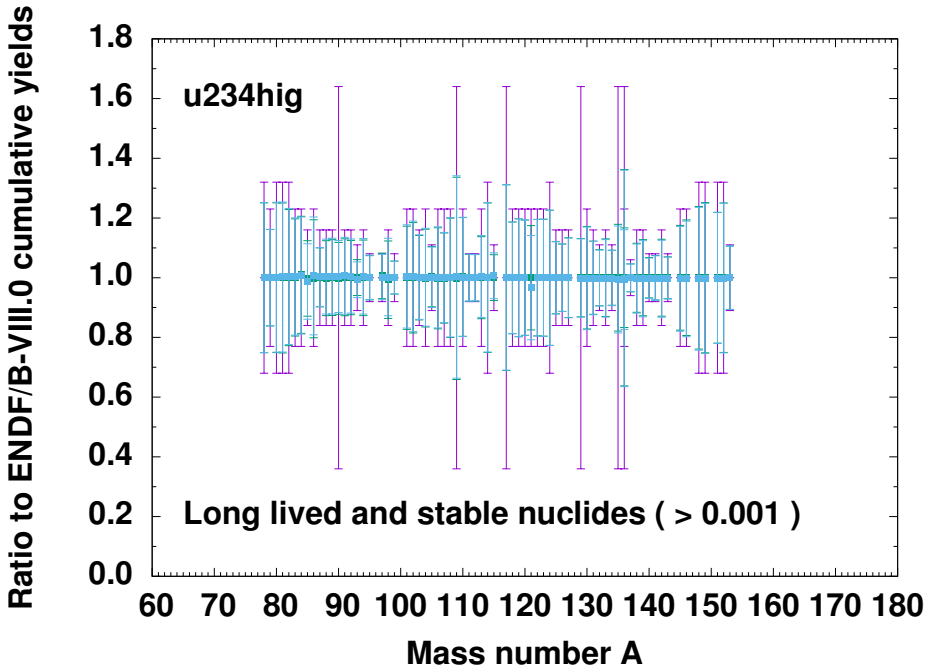

Figure 43. Ratios of adjusted stable and long-lived cumulative yields of magnitude >10^{-3} fitted to ENDF/B-VIII.0 library for ^{234}U at 14 MeV neutron energy.

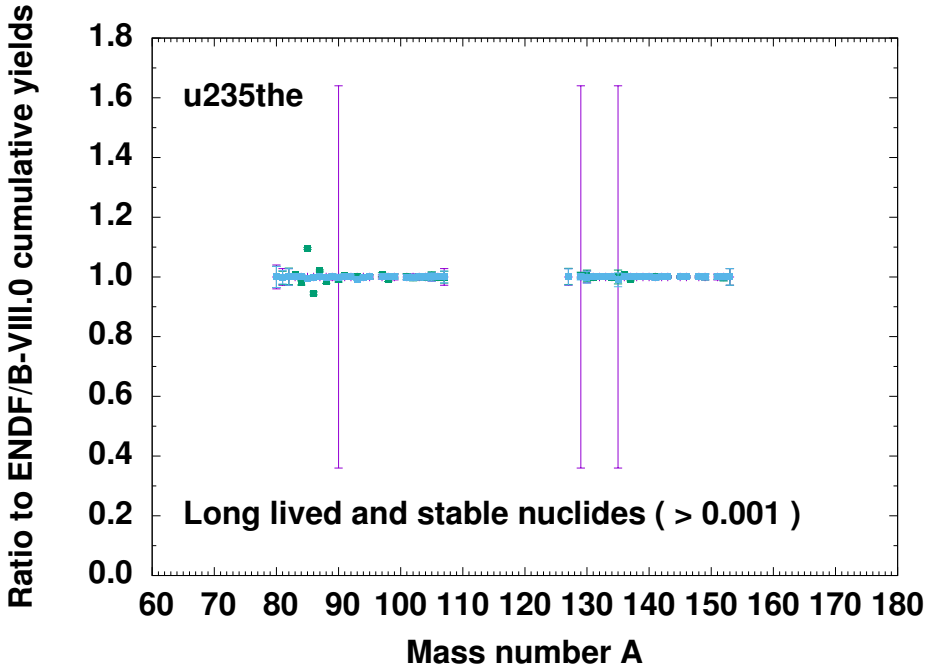

Figure 44. Ratios of stable and long-lived cumulative yields of magnitude $>10^{-3}$ to ENDF/B-VIII.0 library for ^{235}U at thermal neutron energy.

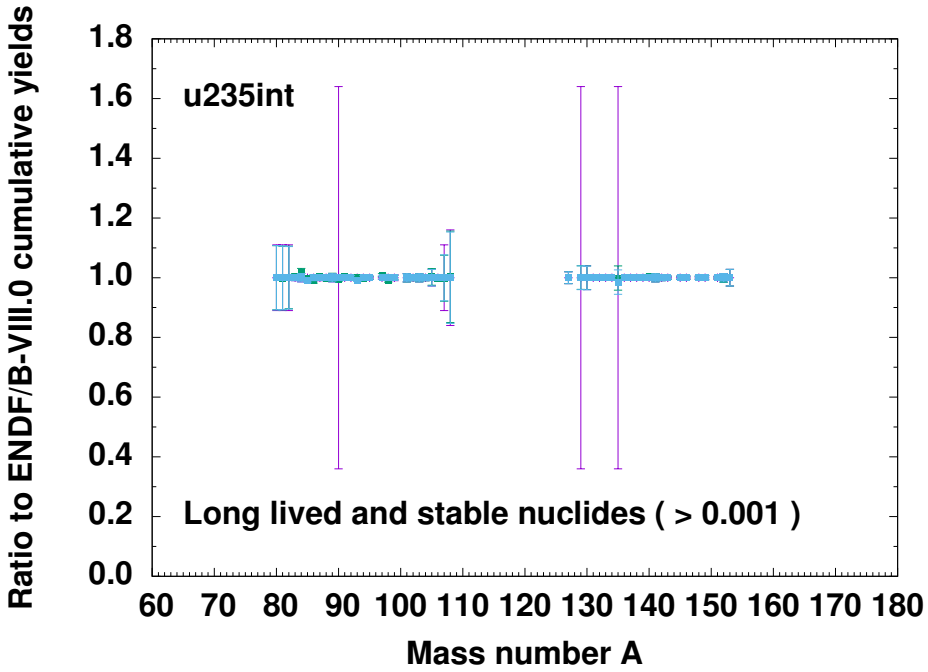

Figure 45. Ratios of stable and long-lived cumulative yields of magnitude $>10^{-3}$ fitted to ENDF/B-VIII.0 library for ^{235}U at 500 keV neutron energy.

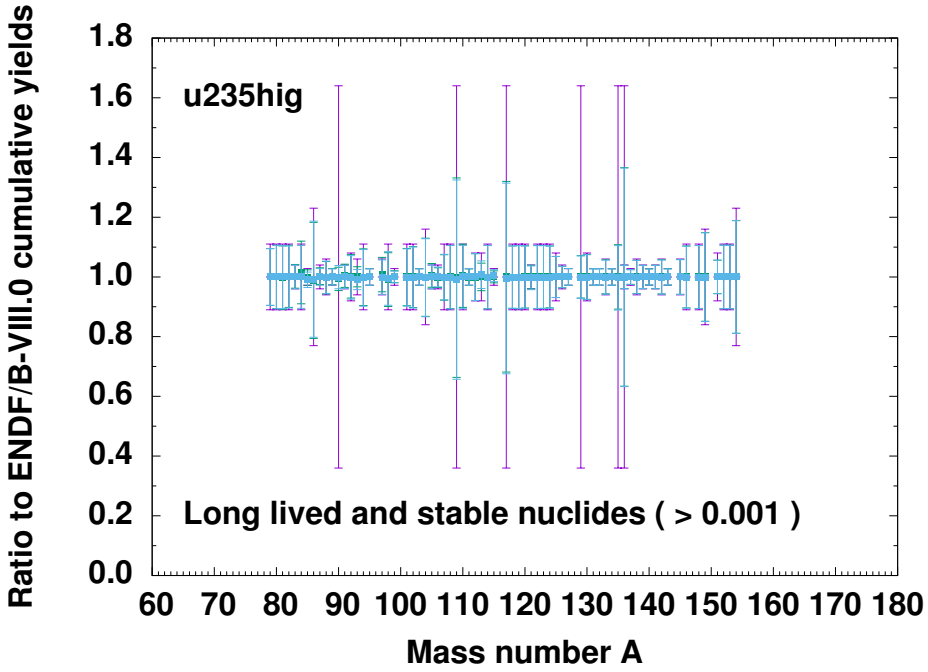

Figure 46. Ratios of adjusted stable and long-lived cumulative yields of magnitude >10^{-3} fitted to ENDF/B-VIII.0 library for ^{235}U at 14 MeV neutron energy.

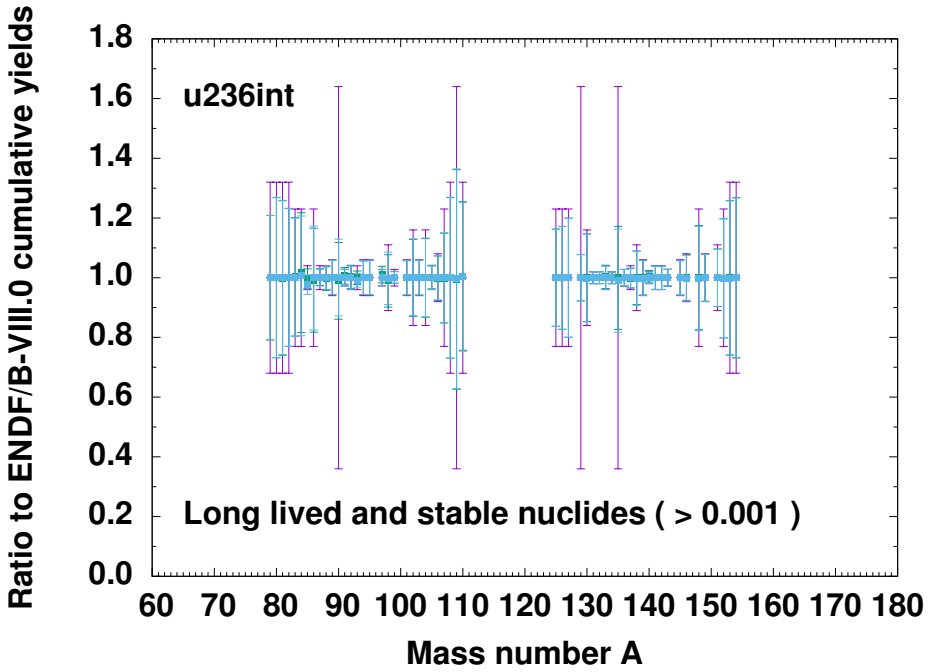

Figure 47. Ratios of stable and long-lived cumulative yields of magnitude >10^{-3} fitted to ENDF/B-VIII.0 library for ^{236}U at 500 keV neutron energy.

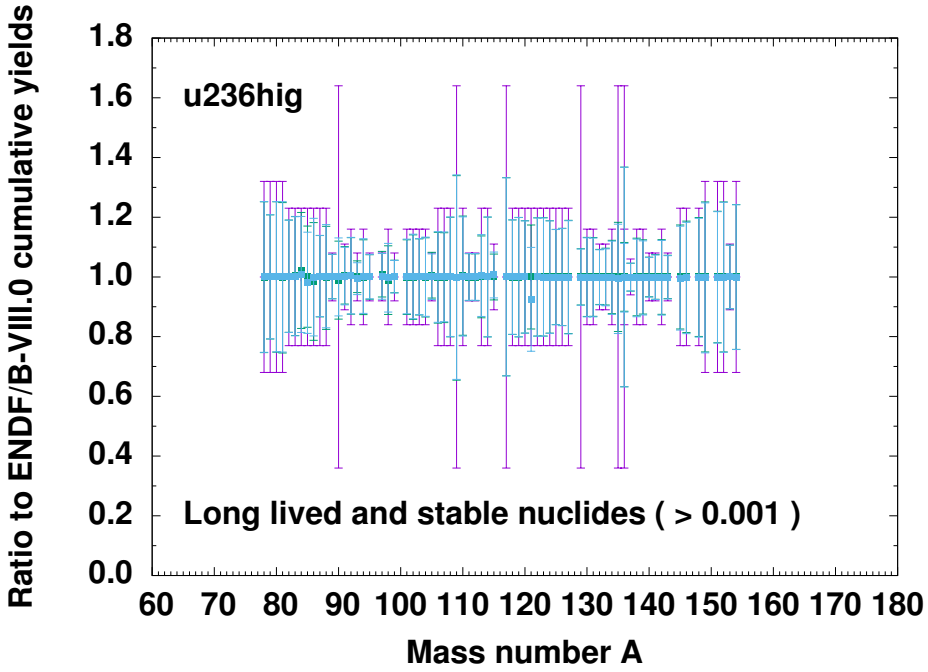

Figure 48. Ratios of stable and long-lived cumulative yields of magnitude $>10^{-3}$ fitted to ENDF/B-VIII.0 library for ^{236}U at 14 MeV neutron energy.

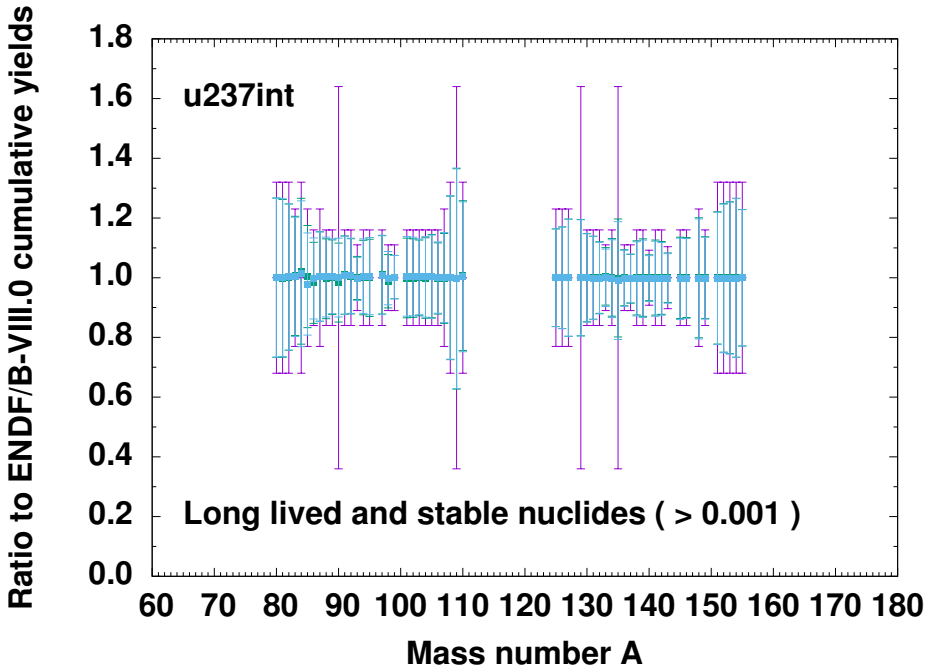

Figure 49. Ratios of stable and long-lived cumulative yields of magnitude $>10^{-3}$ fitted to ENDF/B-VIII.0 library for ^{237}U at 500 keV neutron energy.

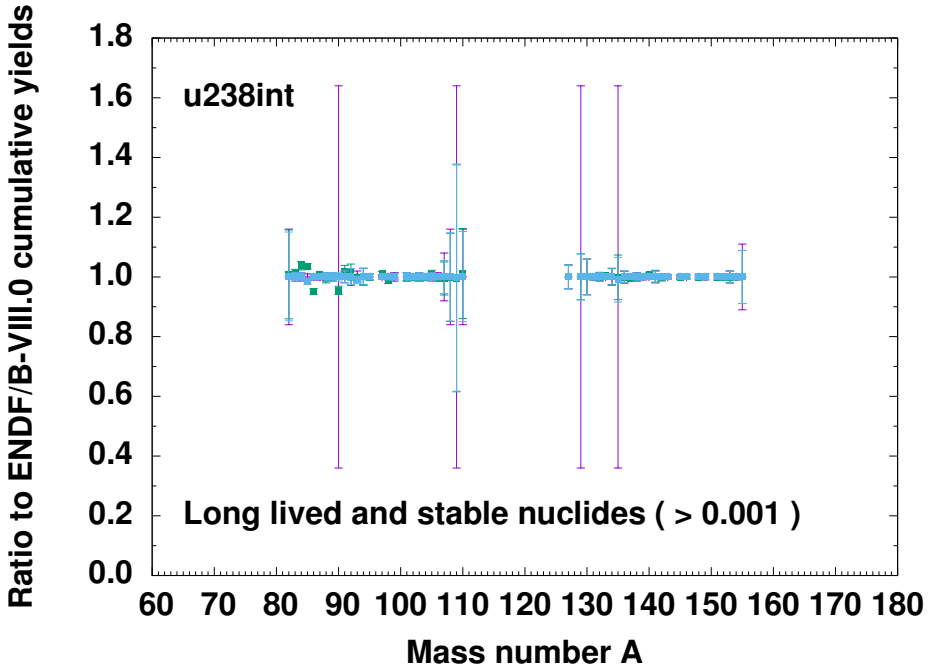

Figure 50. Ratios of stable and long-lived cumulative yields of magnitude $>10^{-3}$ fitted to ENDF/B-VIII.0 library for ^{238}U at 500 keV neutron energy.

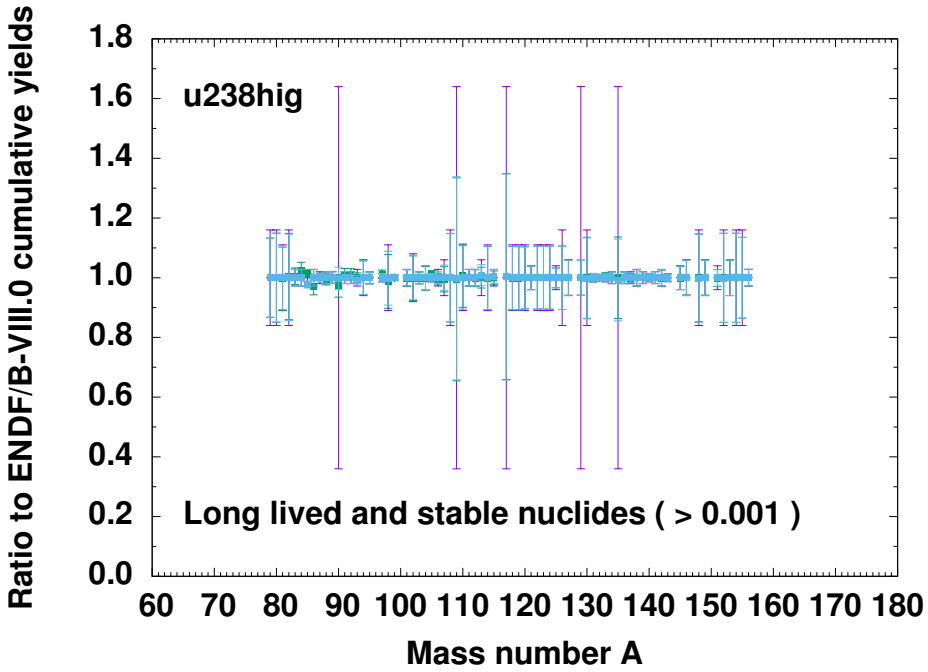

Figure 51. Ratios of stable and long-lived cumulative yields of magnitude $>10^{-3}$ fitted to ENDF/B-VIII.0 library for ^{238}U at 14 MeV neutron energy.

References

[1] M.T. Pigni, M. W. Francis, and I. C. Gauld. Investigation of Inconsistent ENDF/B-VII.1 Independent and Cumulative Fission Product Yields with Proposed Revisions. *Nuclear Data Sheets*, 123, 1 2015.

[2] Matthew W. Francis, Charles F. Weber, Marco T. Pigni, and Ian C. Gauld. Reactor Fuel Isotopics and Code Validation for Nuclear Applications. Technical Report ORNL/TM-2014/464, ORNL, 2 2015.

[3] Marco T. Pigni and Keith C. Bledsoe. Standardizing a Renewed Fission Product Yield Library and Related Covariances (Part I). Technical Report ORNL/TM-2020/1660, ORNL, 9 2020.

[4] Keith C. Bledsoe and Marco T. Pigni. Fission Product Yield Data Adjustment in a Prototype Version of TSURFER. Technical Report ORNL/TM-2021/1939, ORNL, 3 2021.

[5] D.A. Brown, M.B. Chadwick, R. Capote, A.C. Kahler, A. Trkov, M.W. Herman, A.A. Sonzogni, Y. Danon, A.D. Carlson, M. Dunn, D.L. Smith, G.M. Hale, G. Arbanas, R. Arcilla, C.R. Bates, B. Beck, B. Becker, F. Brown, R.J. Casperson, J. Conlin, D.E. Cullen, M.-A. Descalle, R. Firestone, T. Gaines, K.H. Guber, A.I. Hawari, J. Holmes, T.D. Johnson, T. Kawano, B.C. Kiedrowski, A.J. Koning, S. Kopecky, L. Leal, J.P. Lestone, C. Lubitz, J.I. Márquez Damián, C.M. Mattoon, E.A. McCutchan, S. Mughabghab, P. Navratil, D. Neudecker, G.P.A. Nobre, G. Noguere, M. Paris, M.T. Pigni, A.J. Plompen, B. Pritychenko, V.G. Pronyaev, D. Roubtsov, D. Rochman, P. Romano, P. Schillebeeckx, S. Simakov, M. Sin, I. Sirakov, B. Sleaford, V. Sobes, E.S. Soukhovitskii, I. Stetcu, P. Talou, I. Thompson, S. van der Marck, L. Welser-Sherrill, D. Wiarda, M. White, J.L. Wormald, R.Q. Wright, M. Zerkle, G. Žerovnik, and Y. Zhu. ENDF/B-VIII.0: The 8th Major Release of the Nuclear Reaction Data Library with CIELO-project Cross Sections, New Standards and Thermal Scattering Data. *Nuclear Data Sheets*, 148:1 – 142, 2018. Special Issue on Nuclear Reaction Data.

[6] Toshihiko Kawano and Mark B. Chadwick. Estimation of ^{239}Pu independent and cumulative fission product yields from the chain yield data using a Bayesian technique. *Journal of Nuclear Science and Technology*, 50(10):1034–1042, 2013.

[7] T. R. England and B. F. Rider. Evaluation and Compilation of Fission Product Yields 1993. Technical Report LA-UR-94-3106, LANL, 1994.